Quantum invariants and volume of links on surfaces and knotted graphs

David Andrew Will
Richmond, Virginia

Bachelor of Science, Christopher Newport University, 2017

A Thesis presented to the Graduate Faculty
of the University of Virginia in Candidacy for the Degree of
Doctor of Philosophy

Department of Mathematics

University of Virginia
May, 2023

Slava Krushkal, Chair

Sara Maloni

Tom Mark

Israel Klich

Abstract

Since its discovery by Kashaev, the influential Volume Conjecture has attracted much attention towards the ongoing effort of relating diagrammatic and quantum invariants of links in S^3 to the geometry of the link complement. The conjecture has inspired similar open problems which extend it in multiple directions, either to links in more general 3-manifolds or to quantum invariants of other topological objects. This thesis presents contributions to these efforts on both fronts. First, for D a reduced alternating link diagram on a surface Σ, we bound the twist number of D in terms of the coefficients of a polynomial invariant. To this end, we introduce a generalization of the homological Kauffman bracket defined by Krushkal. Combined with work of Futer, Kalfagianni, and Purcell, this yields a bound for the hyperbolic volume of a class of alternating surface links in terms of these coefficients. Second, we prove an instance of Yang's volume conjecture for the relative Turaev–Viro invariants, which are defined for a compact, orientable 3-manifold M via a partially ideal triangulation. We consider the case where M is a punctured S^3 obtained from a knotted trivalent graph Γ belonging to a particular family. We evaluate the limit of relative Turaev–Viro invariants by utilizing techniques relating them to the Reshetikhin–Turaev TQFT and colored Jones polynomials, and we show that this limit equals the volume of O, where O is the outside of Γ, as defined by van der Veen.

Acknowledgments

First and foremost, I am incredibly grateful to my advisor, Slava Krushkal, for all of his wisdom, support, and guidance. I would also like to thank Ilya Kofman and Tian Yang for providing comments which helped improve the contents of this work. Furthermore, I am indebted to the many math teachers who inspired me throughout my life. Most notable among these are my undergraduate professor Mihaela Dobrescu and my high school teacher, the late Todd Phillips. I would also like to thank the friends I made in my cohort at UVA for deepening my love of mathematics and the people who study it. Among these are Reid Booth, Rebecca Claxton, Nick Collins, Aron Daw, and Joe Eisner. Lastly, I would like to thank my mother and my late father for their constant support and encouragement throughout my graduate career.

Contents

1 Introduction

Since its introduction, the Jones polynomial [Jon85] has been of key interest in the ongoing effort to find explicit relations between quantum invariants of a link and the geometry or topology of the link complement. Kashaev's Volume Conjecture [Kas95] posits that such a relationship exists between the colored Jones polynomials, which are an infinite family of invariants generalizing the classical Jones polynomial, and the hyperbolic volume of the link complement. The conjecture in its modern form is stated as follows:

Conjecture 1.1. *[MM01, Conjecture 5.1] Let L be a hyperbolic link and let $J_n(L)$ be the n-th colored Jones polynomial of L evaluated at $q = e^{\frac{\pi i}{n}}$. Then*

$$\lim_{n\to\infty} \frac{2\pi}{n} \ln |J_n(L)| = \mathit{Vol}(S^3 \setminus L). \tag{1}$$

Following its formulation, the conjecture has been verified for several infinite families and stray examples of hyperbolic links (see [Mur11]), though a general proof remains open. The conjecture was extended to encompass all knots and links by means of the Gromov norm, also known as the simplicial volume, in [MM01]. In the subsequent years, the conjecture has been generalized to a variety of settings such as knotted trivalent graphs (KTGs) by van der Veen in [Vee09] and to links in the thickened torus by Boninger in [Bon21]. Moreover, the volume conjecture has inspired similar open problems for related topological invariants such as Chen–Yang's volume conjecture for the Turaev–Viro invariants, a sequence of 3-manifold invariants denoted $TV_r(M)$.

Conjecture 1.2. *[CY18, Conjecture 1.1] Let M be a hyperbolic 3-manifold. Then for r running over odd integers and $TV_r(M)$ evaluated at $q = e^{\frac{2\pi i}{r}}$,*

$$\lim_{r\to\infty} \frac{2\pi}{r} \ln(TV_r(M)) = Vol(M). \tag{2}$$

The volume conjecture and its generalizations are plagued by a common difficulty. Due to the computational complexity of the colored Jones polynomials and related quantum invariants of links, these conjectures have been verified for only a scattering of examples whose quantum invariants are readily known. As an alternative approach to bridging the gap between quantum invariants and volume, Dasbach and Lin [DL07] proved a "volume-ish theorem", which depends only on the classical Jones polynomial as opposed to its colored versions.

Theorem 1.3. *[DL07, Volume-ish Theorem] For an alternating, prime, non-torus knot K, let*

$$V_K(t) = a_n t^n + \cdots + a_m t^m,$$

be the Jones polynomial of K. Then,

$$2v_{tet}(\max(|a_{m-1}|, |a_{n+1}|) - 1) \leq Vol(S^3 \setminus K) \leq 10v_{tet}(|a_{n+1}| + |a_{m-1}| - 1), \tag{3}$$

where $v_{tet} \approx 1.01494$ is the volume of an ideal regular hyperbolic tetrahedron.

This result was obtained in two steps: first, the authors bound the coefficients in terms of the twist number of the link diagram, and second, work of Lackenby, Agol, and Thurston in [Lac04] bounds the volume in terms of the twist number. In a similar fashion to the volume conjecture, an active area of research is focused on extending these steps to more general settings. Futer, Kalfagianni, and Purcell [FKP08] extended

both steps to adequate links, and the latter step has been extended to alternating links in higher-genus surfaces by Kalfagianni and Purcell in [KP20].

1.1 Statement of Results

This thesis contains two main results, both of which fall within this widened realm of the volume conjecture. First, we extend Dasbach–Lin's volume-ish theorem to the setting of reduced alternating links in thickened surfaces. The difficulty, however, is that the classical Jones polynomial does not capture sufficient information about the embedding of links in surfaces. In this paper, we present a new polynomial which is a three-variable generalization of the homological polynomial defined by Krushkal in [Kru11].

Our polynomial, denoted $\langle D \rangle_\Sigma$, is a Laurent polynomial in $\mathbb{Z}[A^{\pm 1}, Z, W]$ defined by a state-sum. Here, A is the usual Kauffman polynomial variable, while Z and W record homological information about the embedding of D on the surface. We will be interested in coefficients of terms having certain fixed degrees in the A variable with minimal degrees in the Z and W variables. The coefficients for the second largest and second smallest degree terms in A are denoted $\alpha'_{(1)}$ and $\beta'_{(1)}$, while those for the third-largest and third-smallest are denoted $\alpha''_{(0)}$ and $\beta''_{(0)}$, respectively. The precise definitions of the polynomial and coefficients are given in Sections 3.2, 4.1. The purpose of the first main theorem is to extend the volume-ish theorem to the setting of links in thickened surfaces by bounding these coefficients in terms of the twist number, generalizing the method in [FKP08].

Main Theorem 1. *Let Σ be a closed, orientable surface and let D be a reduced alternating link diagram on Σ such that every twist region of D has at least three crossings. Let $\star = \alpha'_{(1)} + \beta'_{(1)} - \alpha''_{(0)} - \beta''_{(0)} + 2$. Then,*

$$\frac{1}{3}tw(D) + 1 - g(\Sigma) \leq \star \leq 2tw(D). \tag{4}$$

Combined with the result in [KP20], Main Theorem 1 yields the following volume bounds.

Corollary 1.4. *Let Σ be a closed orientable surface of genus at least one, and let L be a link that admits a twist-reduced weakly generalized cellularly embedded alternating projection D onto $\Sigma \times \{0\}$ in $Y = \Sigma \times [-1, 1]$. Then the interior of $Y \setminus L$ admits a hyperbolic structure. If Σ is a torus, then we have*

$$\frac{v_{oct}}{4}\star \leq \mathit{Vol}(Y \setminus L) < 30v_{tet}\star, \tag{5}$$

where $v_{tet} \approx 1.01494$ is the volume of a regular ideal tetrahedron, and $v_{oct} \approx 3.66386$ is the volume of a regular ideal octahedron.

If Σ has genus at least two, then we have

$$\frac{v_{oct}}{4} \cdot (\star - 6\chi(\Sigma)) \leq \mathit{Vol}(Y \setminus L) < 18v_{oct} \cdot (\star + g(\Sigma) - 1). \tag{6}$$

The second main result deals with Chen–Yang's conjecture for the Turaev–Viro invariants, or more precisely, a relative version of the invariants defined by Yang in [Yan21]. The relative invariants, denoted by $TV_r(M, \mathcal{T}, \mathbf{b}^{(r)})$, are defined for a compact, oriented 3-manifold M with a partially ideal triangulation $\mathcal{T}$ whose edges are colored by the sequence $\mathbf{b}^{(r)}$. The precise definitions of these parameters are found in

Section 5.2. Attempts to directly verify either Conjecture 1.2 or Yang's corresponding conjecture for the relative invariants (Conjecture 5.14 in this paper) are hindered by the sheer computational complexity of the quantum ingredients which comprise the Turaev–Viro invariants. Detcherry, Kalfagianni, and Yang [DKY18] identified the first examples satisfying Conjecture 1.2, where M is chosen to be the complement of the figure-eight knot or Borromean rings. They do so by re-expressing the Turaev–Viro invariants of M in terms of the colored Jones polynomials of the link, which are readily known for these examples. In the second main theorem, we extend their methods to the relative setting, but the natural choice of the manifold M in this setting is no longer a link complement. Rather, it is a manifold related to the "outside" of a knotted trivalent graph (KTG), the analogue of a link complement for KTGs introduced by van der Veen [Vee09].

In addition to having outsides, the notion of a colored Jones polynomial also extends to the setting of KTGs. The colored Jones evaluation of a KTG Γ is denoted by $\langle \Gamma \rangle_{\mathbf{i}}$, where $\mathbf{i}$ is a sequence of colors on the edges of Γ, and is akin to the colored Jones polynomial of Γ. Given a KTG in S^3, one may obtain an "augmented" version of it as defined in [Vee09]. These augmented KTGs are designed with the express purpose of having hyperbolic outsides with volumes which are easy to compute, not unlike the simple links used in [DKY18] to study Conjecture 1.2. Augmented KTGs also have the benefit of having colored Jones evaluations which are more easily expressed than those of ordinary KTGs. Both the notions of augmented KTGs and outsides will be discussed in greater detail in Section 5.5. By using this augmented KTG to choose a particular manifold M, a triangulation $\mathcal{T}$, and colorings $\mathbf{b}^{(r)}$, we show that one may compute $TV_r(M, \mathcal{T}, \mathbf{b}^{(r)})$ in terms of particular evaluations of Γ, which we denote by $\langle \Gamma \rangle_{\mathbf{i},n}$. The result is stated as follows:

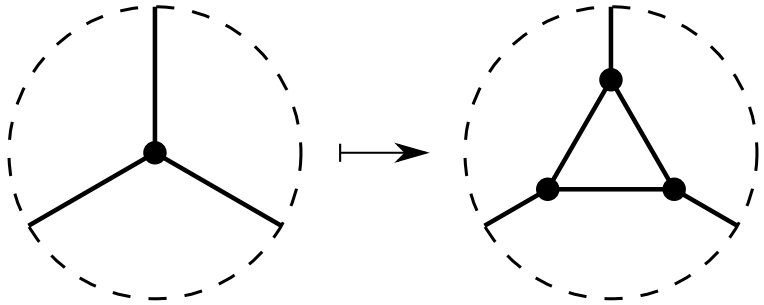

Figure 1: The triangle move.

Main Theorem 2. *Let $r \geq 9$ be an odd integer and $\Gamma \subset S^3$ an augmented KTG with v_Γ vertices. Let M, $\mathcal{T}$, and $\boldsymbol{b}^{(r)}$ be defined as in Section 6.1, and let v_{inn} be the number of inner vertices of $\mathcal{T}$. Then,*

$$TV_r(M, \mathcal{T}, \boldsymbol{b}^{(r)}) = 2^{v_\Gamma + v_{inn} - 1} (\eta'_r)^{2-2v_\Gamma} \theta(n,n,n)^{-v_\Gamma} [n+1]^{-v_{inn}} \sum_{\substack{0 \leq \boldsymbol{i} \leq r-3, \\ \boldsymbol{i} \text{ even}}} |\langle \Gamma \rangle_{\boldsymbol{i},n}|^2 , \quad (7)$$

where $\eta'_r = \frac{2\sin(\frac{2\pi}{r})}{\sqrt{r}}$, and $\langle \Gamma \rangle_{\boldsymbol{i},n}$ is the colored Jones evaluation of Γ where the augmentation rings are colored by $\boldsymbol{i} = (i_1, \ldots, i_{|A|})$ and all other edges by n.

By applying this result to a special family of augmented KTGs, we are able to verify the relative version of the Chen–Yang conjecture for a particular choice of $(M, \mathcal{T}, \mathbf{b}^{(r)})$. The KTGs in question are precisely those which can be obtained from the tetrahedron graph by a finite sequence of "triangle moves" (see Figure 1). These are a special instance of augmented KTGs having zero augmentation rings. In other words, we will prove the following corollary:

Corollary 1.5. *Let $\Gamma \subset S^3$ be a KTG which can be generated from the tetrahedron graph using t triangle moves (and some number of half-twist moves, which change the framing of an edge), and let M, $\mathcal{T}$, and $\boldsymbol{b}^{(r)}$ be defined as in Section 6.1. Then,*

$$\lim_{r\to\infty} \frac{2\pi}{r} \log(TV_r(M, \mathcal{T}, \boldsymbol{b}^{(r)})) = (2t+2)v_{oct} = Vol(O_\Gamma), \tag{8}$$

where O_Γ is the "outside" manifold of Γ, as defined in [Vee09]. Thus, the relative Chen–Yang conjecture (Conjecture 5.14 in this paper) holds for $(M, \mathcal{T}, \boldsymbol{b}^{(r)})$.

1.2 Layout of Thesis

We begin with a brief introduction of hyperbolic geometry in Section 2. The remainder of the thesis is split into two halves, each focusing on one of the main theorems. Section 3 contains background details for Main Theorem 1. It is divided into Section 3.1 covering links in thickened surfaces, Section 3.2 containing the definition of the polynomial $\langle D \rangle_\Sigma$, and Section 3.3 on state graphs, which will play a key role in the proof to come. Section 4 contains the proof of Main Theorem 1, which is split into two parts. First, in Section 4.1 we define the coefficients $\alpha'_{(1)}$, $\beta'_{(1)}$, $\alpha''_{(0)}$, and $\beta''_{(0)}$ and compute them in terms of combinatorial information coming from the state graphs. Second, in Section 4 we employ a variety of homological arguments to bound these quantities in terms of the twist number of the diagram D and the genus of the surface Σ. The proof is followed by a brief discussion in Section 4.3, which compares Main Theorem 1 to related results.

The second half of the thesis focuses on Main Theorem 2 and is structured in much the same way. Section 5 contains background details for several different quantum invariants which will be used in the proof. We begin with Section 5.1 where we use

skein theory to define the Jones–Wenzl projectors and state the definition of the colored Jones evaluation of a KTG. With this foundation, we define the relative Turaev–Viro invariants in Section 5.2 and the Reshetikhin–Turaev invariants in Section 5.3, where we also prove a result relating the two. In the proof, we will also make use of the Reshetikhin–Turaev topological quantum field theory (TQFT), which is covered in Section 5.4. Lastly, in Section 5.5, we define KTGs, their outsides, and augmentation, all of which are centrally important to Main Theorem 2 and its corollaries. Section 6 is devoted to the proof of Main Theorem 2. In Section 6.1, we start by defining the quantities M, $\mathcal{T}$, and $\mathbf{b}^{(r)}$ and proceed with the proof. This is followed by the proof of Corollary 1.5 in Section 6.2 and a discussion in Section 6.3.

2 Background on hyperbolic geometry

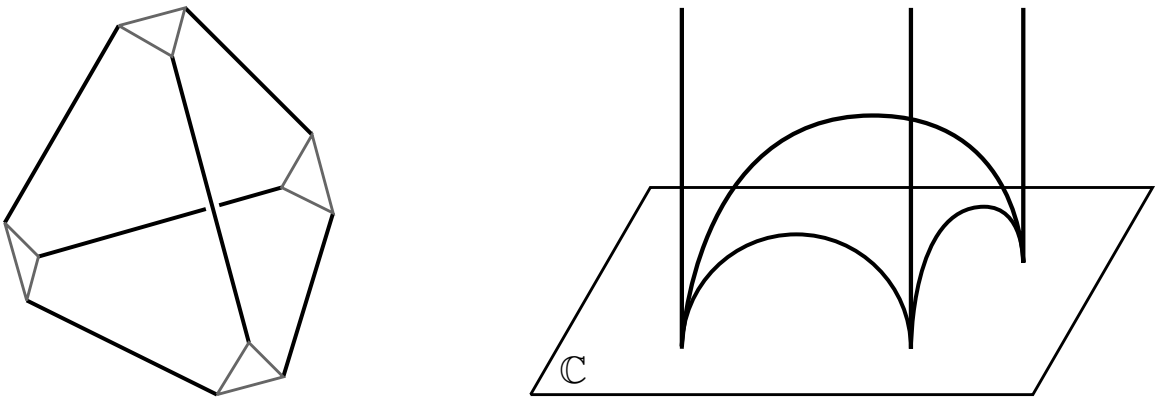

Figure 2: Left: A truncated tetrahedron. Right: An ideal tetrahedron in $\mathbb{H}^3$.

As previously discussed, the main theorems of this paper have applications to hyperbolic geometry when combined with results from the literature. For this reason, we start with some basic definitions and terminology. The details of this section can all be found in [Thu97] and [Pur20].

Hyperbolic 3-space, denoted $\mathbb{H}^3$, is defined to be the upper half-space $\{(x+iy,t) \in \mathbb{C}\times\mathbb{R} \mid t>0\}$ equipped with the metric $ds^2 = \frac{dx^2+dy^2+dt^2}{t^2}$. A key feature of $\mathbb{H}^3$ is the *boundary at infinity*, $\partial\mathbb{H}^3 = \mathbb{C}\cup\{\infty\}$ which is infinitely far away from any point in $\mathbb{H}^3$. Under this upper half-space model, the geodesics are lines or semicircles intersecting $\mathbb{C}$ transversely at right angles, and the isometries uniquely correspond to elements of $PSL(2,\mathbb{C})$.

Ideal polyhedra are the building blocks of hyperbolic manifolds. An *ideal polyhedron* $P \subset \mathbb{R}^3$ is a Euclidean polyhedron whose vertices are truncated by the removal of small closed neighborhoods. We refer to the new edges and faces produced by this as truncation edges and truncation faces, respectively, which can be seen in Figure 2. When an ideal polyhedron P is embedded in $\mathbb{H}^3$, we send the truncation faces to $\partial\mathbb{H}^3$ and arrange for the non-truncation faces to be totally geodesic so that P inherits

the hyperbolic metric. A *hyperbolic 3-manifold* is a 3-manifold M with local charts (U, ϕ), where ϕ is a map $\phi : U \subset M \to \phi(U) \subset \mathbb{H}^3$, such that the transition maps are hyperbolic isometries. The simplest way to show that a manifold admits a hyperbolic structure is to decompose M into ideal polyhedra and let the open neighborhoods U be the interiors of these polyhedra. Then one only needs to check that after the polyhedra are embedded in $\mathbb{H}^3$, the face pairings are isometries. This condition is encapsulated by Thurston's edge gluing equations [Pur20, Theorem 4.7] which demand that the sum of dihedral angles around any given edge is 2π.

Whether or not the hyperbolic structure on a given manifold is complete depends on whether a second collection of edge gluing equations given by Thurston is satisfied [Pur20, Theorem 4.10]. One tactic used in the literature to show that a given manifold has a complete hyperbolic structure, which will be referenced in Section 5.5, is to let the polyhedral decomposition consist solely of regular ideal octahedra glued in pairs, which trivially satisfy the gluing equations.

For a hyperbolic manifold M, the boundary of M is comprised of the truncation faces sent to $\partial\mathbb{H}^3$ along with any unglued totally geodesic faces. A *cusp* of a hyperbolic manifold is a regular neighborhood of the truncation faces. If M is complete, the hyperbolic structure induces a Euclidean structure on the boundary of cusps. Consequently, orientable complete hyperbolic manifolds can only have toroidal or annular cusped boundary components. This makes link complements some of the simplest manifolds which can admit complete hyperbolic structures, and we refer to a link with such a complement as *hyperbolic*. Indeed, as a consequence of Thurston's hyperbolization theorem, all knots can be classified as either torus, satellite, or hyperbolic [Thu82, Corollary 2.5], and most prime knots with up to 19 crossings are hyperbolic [Bur].

Another classical result which is paramount to the study of hyperbolic links is Mostow–Prasad rigidity.

Theorem 2.1. *[Pra73] Let M_1 and M_2 be complete hyperbolic n-manifolds, $n \geq 3$ with finite volume. Then any isomorphism of fundamental groups $\phi : \pi_1(M_1) \xrightarrow{\sim} \pi_1(M_2)$ is realized by a unique isometry.*

As a consequence, if M is the complement of a hyperbolic link L, then we may think of its hyperbolic structure (and by extension, any well-defined feature of said structure) as a geometric link invariant. In particular, we may consider $Vol(M)$ which we refer to simply as the *hyperbolic volume* of L.

3 Quantum invariants of links in thickened surfaces

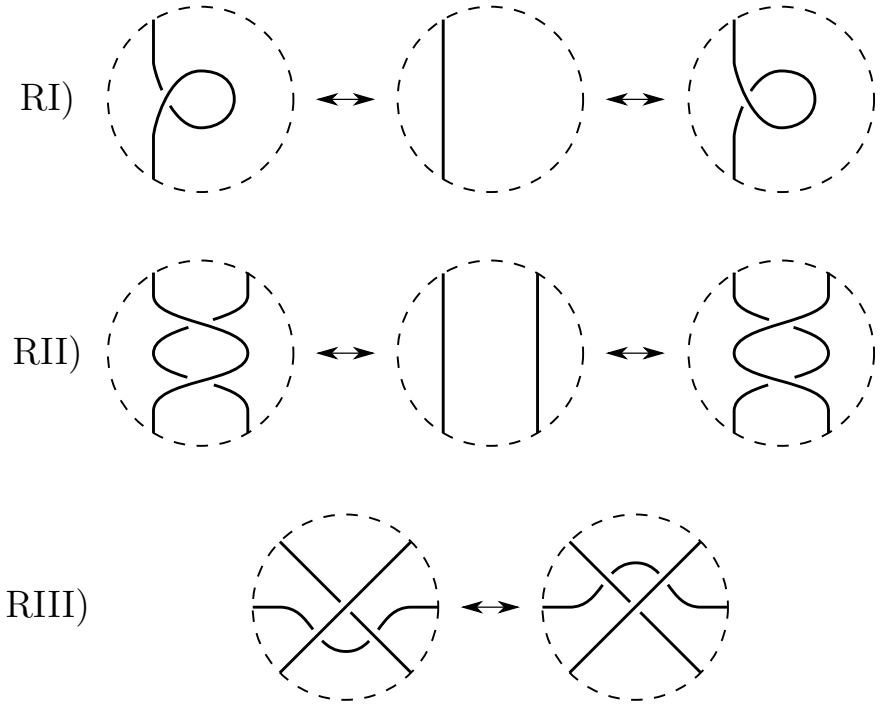

Figure 3: The Reidemeister moves.

3.1 Links in thickened surfaces

Definition 3.1. A *link* L in a 3-manifold M is a smooth embedding of circles $\bigsqcup_{i=1}^{k} S^1_{(i)} \hookrightarrow M$. Here, k is the number of components of the link.

Throughout Sections 3 and 4, we will let Σ be a closed, orientable surface and we will let M be $\Sigma \times [-1, 1]$. We will implicitly view Σ as $\Sigma \times \{0\} \subset M$, but since these sections deal primarily with link diagrams, these results will hold for Σ in any compact, orientable, irreducible 3-manifold. Links are considered up to isotopy, or smooth deformation.

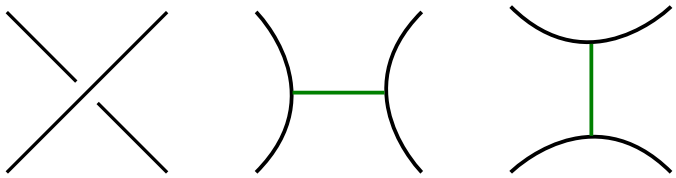

Figure 4: A crossing, an A-resolution, and a B-resolution.

Definition 3.2. For a link $L \subset \Sigma \times [-1, 1]$, a *link diagram* D for L on Σ is the image of L under the projection $\Sigma \times [-1, 1] \twoheadrightarrow \Sigma$, which we may view as a 4-valent graph Γ on Σ. The vertices of Γ correspond to double points of the projection. These vertices are then equipped with crossing information which denotes the relative heights of the two points in the preimage.

A classical theorem of Reidemeister, which also holds for links in thickened surfaces, states that two links are isotopic if and only if their diagrams differ by a sequence of Reidemeister moves, seen in Figure 3, as well as planar isotopy.

There are two possible ways to resolve each crossing. Resolving a crossing means replacing D with a new diagram having one fewer crossing which differs from D only in a neighborhood of that crossing. We call these the A-resolution and the B-resolution, referring to Figure 4. As we resolve crossings, we may draw an arc connecting the strands of the new diagram. These are commonly called "surgery arcs," as performing surgery along such an arc provides a convenient way to switch between the A and B resolutions of a crossing.

If all crossings are resolved, then all that remains of D is a collection S of disjoint simple closed curves on Σ. We call S a *state*, and denote the set of all states by $\mathcal{S}$. Note that $|\mathcal{S}| = 2^{c(D)}$ where $c(D)$ is the number of crossings of D.

We will be considering only link diagrams which are alternating and reduced. A link diagram on a surface is *reduced* if it is cellularly embedded and if it contains no

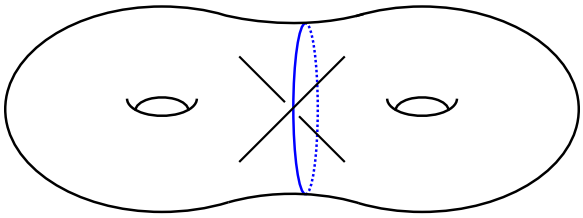

Figure 5: A nugatory crossing.

nugatory crossings. By cellularly embedded, we mean that the complementary regions of the graph Γ are disks. A crossing is *nugatory* if there exists a separating curve in Σ that intersects D only at that crossing as in Figure 5.

3.2 Definition of the polynomial

The polynomial we will be studying is a generalization of the homological Kauffman bracket, defined by Krushkal in [Kru11]. Let $i : S \to \Sigma$ be the inclusion map. "Homological" refers to the use of the induced map $i_* : H_1(S) \to H_1(\Sigma)$, which provides additional information about the embedding of each state. Throughout this paper, we use $\mathbb{Z}$ coefficients unless otherwise indicated.

Definition 3.3. [Kru11] Let $\alpha(S)$ and $\beta(S)$ respectively denote the number of A-resolutions and B-resolutions used to obtain the state S. The *homological Kauffman bracket* is a Laurent polynomial $\langle D\rangle_{\Sigma}^{H} \in \mathbb{Z}[A^{\pm 1}, Z]$ defined by the state-sum

$$\langle D\rangle_{\Sigma}^{H} = \sum_{S\in\mathcal{S}} A^{\alpha(S)-\beta(S)}(-A^2 - A^{-2})^{k(S)} Z^{r(S)}, \tag{9}$$

where

$$k(S) = \dim(\ker\{i_* : H_1(S) \to H_1(\Sigma)\}),$$
$$r(S) = \dim(\mathrm{im}\{i_* : H_1(S) \to H_1(\Sigma)\}).$$

Here $k(S)$ is called the *kernel* of the state, while $r(S)$ is called the *homological rank* of the state. We write

$$\langle D \mid S\rangle_{\Sigma}^{H} = A^{\alpha(S)-\beta(S)}(-A^2 - A^{-2})^{k(S)} Z^{r(S)}, \tag{10}$$

for the contribution of the state S to $\langle D\rangle_{\Sigma}^{H}$.

The proof that $\langle D\rangle_{\Sigma}^{H}$ yields an invariant of links in thickened surfaces will follow from the proof of invariance for $\langle D\rangle_{\Sigma}^{H}$, which is given below. For alternating links, [Thi87] shows that the classical Jones polynomial can be viewed as a specialization of the Tutte polynomial for a related graph. In [Kru11], a homological version of the Tutte polynomial is defined for surface graphs, and then the homological Kauffman bracket is obtained as a specialization of the graph polynomial. More recently, in [FK22], Fendley and Krushkal define a more general version of this graph polynomial for graphs on the torus. More specifically, for a graph with homological rank equal to one, a third variable W is introduced which counts the number of components of the graph which are homologically essential. Inspired by this generalization, we present a version of this polynomial for link diagrams and extend it to higher-genus surfaces.

Definition 3.4. Define $\bar{c}(S)$ to be zero if $r(S) \neq 1$. If $r(S) = 1$, then define $\bar{c}(S)$ to be one-half the number of homologically essential loops in S. The more general homological Kauffman bracket which will be used throughout this paper is given by

$$\langle D\rangle_{\Sigma} = \sum_{S\in\mathcal{S}} A^{\alpha(S)-\beta(S)}(-A^2 - A^{-2})^{k(S)} Z^{r(S)} W^{\bar{c}(S)}, \tag{11}$$

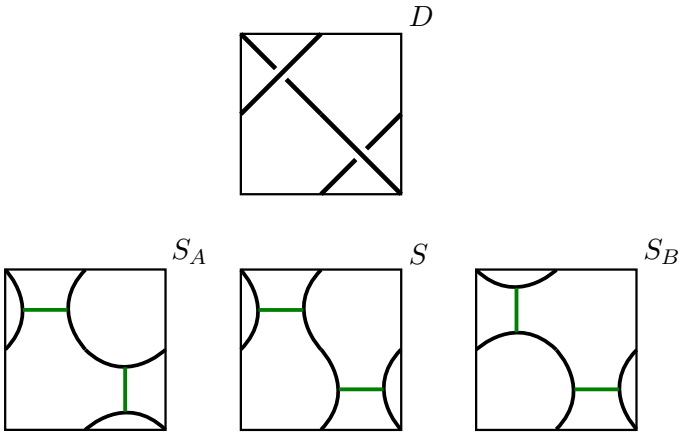

Figure 6: Top: A link diagram on the torus. Bottom: The all-A state S_A, one of two intermediate states, and the all-B state S_B.

and we similarly write

$$\langle D \mid S \rangle_\Sigma = A^{\alpha(S)-\beta(S)}(-A^2 - A^{-2})^{k(S)} Z^{r(S)} W^{\bar{c}(S)}, \tag{12}$$

for the contribution of a state.

Example 3.5. As an example, consider the two component link diagram D in the torus depicted in Figure 6. For the all-A and all-B states, we can see that $k(S_A) = k(S_B) = 1$ and $r(S_A) = r(S_B) = 0$. For the two remaining intermediate states, which differ by diagonal reflection, we have that $k(S) = 1$ and $r(S) = 1$ for both. Furthermore, each intermediate state has exactly two homologically essential loops, so $\bar{c}(S) = 1$. This yields $\langle D \rangle_\Sigma = -A^4 - 2A^2ZW - 2 - 2A^{-2}ZW - A^{-4}$.

Remark 3.6. The terms of second/third largest/smallest degree in the A variable referenced in the definition of $\star$ refer to the possible degrees of A, so that coefficients taking the value zero are allowed. These possible terms are described explicitly in Propositions 4.5 and 4.8 in Section 4.1. Terms are also allowed to coincide. For instance, in Example 3.5 the third smallest and third largest degree terms are both -2.

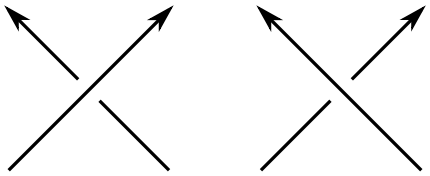

Figure 7: A positive crossing and a negative crossing.

To show that a quantity is an invariant of links in thickened surfaces, it suffices to check invariance under the Reidemeister moves in Figure 3. Since the Reidemeister moves are local in nature, taking place in disks contained in Σ, the following argument is identical to the one commonly seen in the classical planar setting. As in that case, we can see here that $\langle\cdot\rangle_\Sigma$ is invariant under RII by computing

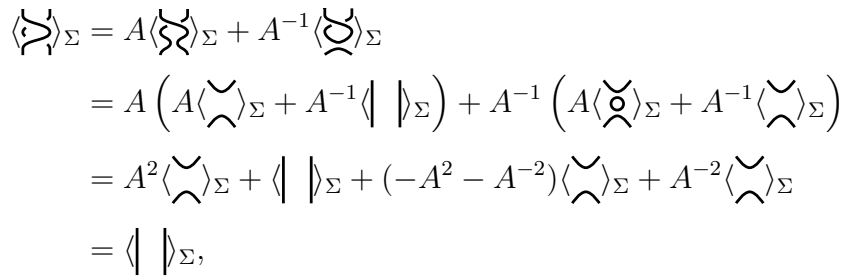

and the argument that $\langle \; | \; | \; \rangle_\Sigma = \langle \; \rangle\!\langle \; \rangle_\Sigma$ is completely symmetrical. Invariance under RIII follows from invariance under RII and planar isotopy by observing

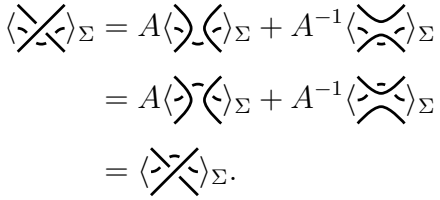

Presently, $\langle\cdot\rangle_\Sigma$ is not invariant under RI since $\langle$  $\rangle_\Sigma = -A^3\langle \; | \; \rangle_\Sigma$ and $\langle$ 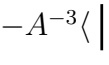 $\rangle_\Sigma = -A^{-3}\langle \; | \; \rangle_\Sigma$. However, this can be rectified by orienting D and observing that RI alters the writhe of D. The *writhe* of an oriented diagram is defined by

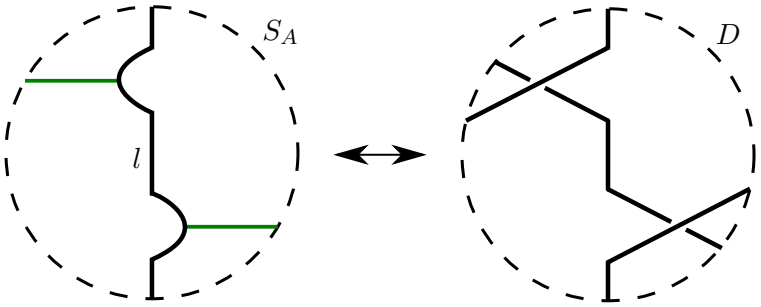

Figure 8: Arcs on opposite sides of l contradict the fact that D is alternating.

$w(D) = c_+(D) - c_-(D)$, where $c_+(D)$ and $c_-(D)$ are the numbers of positive and negative crossings, respectively (see Figure 7). To obtain invariance under the first Reidemeister move, a homological version of the Jones polynomial may be obtained by setting

$$J_\Sigma(t, Z, W) = (-A)^{-3w(D)} \langle D \rangle_\Sigma \big|_{A=t^{-\frac{1}{4}}}. \tag{13}$$

Note that the substitution and renormalization of 13 do not affect the polynomial coefficients, so $\langle D \rangle_\Sigma$ will suffice for our purposes.

Remark 3.7. In [BK22b, Proposition 1.7], the authors note that any checkerboard colorable link L bounds an unoriented surface embedded in $\Sigma \times I$, namely, either the white or black checkerboard surface obtained by attaching half-twisted bands to the white or black regions, respectively. Therefore, $[L] = 0$ in $H_1(\Sigma \times [-1, 1]; \mathbb{Z}_2)$. Under the projection, L is $\mathbb{Z}_2$-homologous to the sum of all loops in any fixed state S. Thus, $[S] = 0$ in $H_1(\Sigma; \mathbb{Z}_2)$ as well. As a result, if $r(S) = 1$, then there must be an even number of essential loops in S, so we conclude that $\langle D \rangle_\Sigma \in \mathbb{Z}[A^{\pm 1}, Z, W]$ for checkerboard colorable diagrams. In particular, since alternating, cellularly embedded link diagrams are checkerboard colorable by [BK22b], this will hold for the class of links considered in Theorem 1.

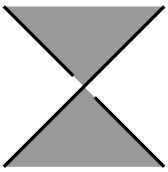

Figure 9: A crossing of a checkerboard colorable diagram.

3.3 State graphs and the twist number

Let S_A denote the all-A state, and let S_B denote the all-B state, each obtained by selecting only that type of resolution. If D is alternating, and l is any loop in either S_A or S_B, then all surgery arcs attached to l must lie on the same side of l as seen in Figure 8. For $S \in \mathcal{S}$, let $\mathcal{A}(S)$ denote the collection of surgery arcs for S. Consider $U = S \cup \mathcal{A}(S)$. Observe that we can recover the underlying 4-valent graph Γ by contracting each arc of U to a point. This contraction induces a homeomorphism between the complementary regions of U and the complementary regions of Γ. Therefore, if D is cellularly embedded, the complementary regions of U must be disks. As a result, the side of l containing no edges must be one of these disk regions. In other words, every loop of S_A and S_B is contractible. Therefore, we can use the states S_A and S_B to define the following graphs on Σ.

Definition 3.8. The *all-A state graph* $\mathbb{G}_A$ is a graph embedded on Σ whose vertices correspond to the loops of S_A and whose edges correspond to the surgery arcs seen in Figure 4. The *all-B state graph* $\mathbb{G}_B$ is defined similarly for S_B.

Remark 3.9. Note that as a consequence, we can conclude that reduced alternating diagrams are *checkerboard colorable*, i.e., that the complementary regions can be colored white and black so that every vertex appears as in Figure 9. We simply color regions containing vertices of $\mathbb{G}_A$ white and regions containing vertices of $\mathbb{G}_B$ black.

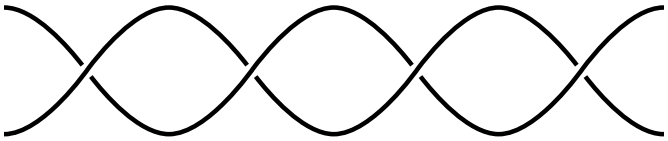

Figure 10: A twist region.

Our goal will be to express certain coefficients of $\langle D \rangle_\Sigma$ in terms of combinatorial information coming from $\mathbb{G}_A$ and $\mathbb{G}_B$. This will enable us to form a connection between the coefficients and the twist number of D.

Definition 3.10. Let D be a reduced link diagram on a surface Σ. By definition, the complementary regions of D are n-gons with $n \geq 2$. A *twist region* is a connected sequence of bigons arranged crossing-to-crossing of maximal length, as in Figure 10. A single crossing which is adjacent to no bigon regions is also considered to be a twist region.

Definition 3.11. A reduced diagram D on Σ is *twist-reduced* if for any disk E meeting D transversely in four points adjacent to two crossings as in Figure 11, either E contains a (possibly empty) sequence of bigons, or there exists a disk E' in $\Sigma \setminus E$ adjacent to the same two crossings which contains a (possibly empty) sequence of bigons.

The number of twist regions of a twist-reduced diagram D is called the *twist number* of D and is denoted $tw(D)$.

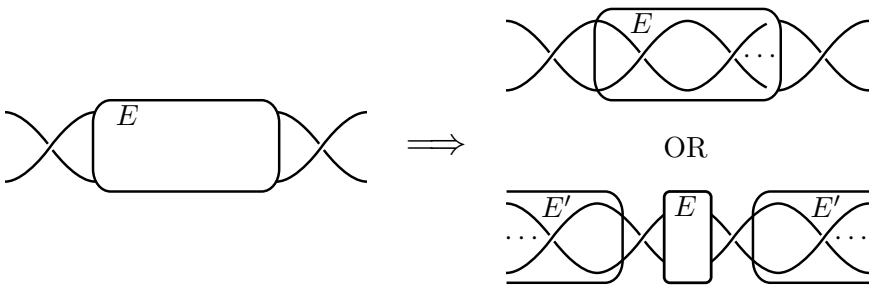

Figure 11: A twist-reduced diagram.

4 Proof of Main Theorem 1

The goal of this section is to express certain coefficients of $\langle D \rangle_\Sigma$ in terms of combinatorial information coming from $\mathbb{G}_A$ and $\mathbb{G}_B$. In Section 4.2, this combinatorial information will lead to a proof of Main Theorem 1, which we restate here for the convenience of the reader.

Main Theorem 1. *Let Σ be a closed, orientable surface and let D be a reduced alternating link diagram on Σ such that every twist region of D has at least three crossings. Let $\star = \alpha'_{(1)} + \beta'_{(1)} - \alpha''_{(0)} - \beta''_{(0)} + 2$. Then,*

$$\frac{1}{3}tw(D) + 1 - g(\Sigma) \leq \star \leq 2tw(D). \tag{4}$$

4.1 Computation of coefficients

Let v_A and v_B denote the number of vertices in $\mathbb{G}_A$ and $\mathbb{G}_B$ (alternatively, the number of loops in S_A and S_B), respectively. Since all the loops in S_A and S_B are contractible, they are homologically trivial. This shows the states S_A and S_B contribute

$$\langle D \mid S_A \rangle_\Sigma = A^{c(D)}(-A^2 - A^{-2})^{v_A}, \tag{14}$$

$$\langle D \mid S_B \rangle_\Sigma = A^{-c(D)}(-A^2 - A^{-2})^{v_B}, \tag{15}$$

to $\langle D \rangle_\Sigma$. For a polynomial $p \in \mathbb{Z}[A^{\pm 1}, Z, W]$, we write $\deg^A_{\max}(p)$ and $\deg^A_{\min}(p)$ for the maximal and minimal degrees of p in the variable A, respectively. Note from the above, that

$$\deg^A_{\max}\langle D \mid S_A\rangle_\Sigma = c(D) + 2v_A, \tag{16}$$

$$\deg^A_{\min}\langle D \mid S_B\rangle_\Sigma = -c(D) - 2v_B. \tag{17}$$

In fact, these degrees are precisely the maximal and minimal degrees in A of the polynomial $\langle D\rangle_\Sigma$. Boden and Karimi show this for $\langle D\rangle^H_\Sigma$ in [BK22b, Proposition 2.8] by proving that reduced alternating diagrams on surfaces are homologically adequate. We summarize their definition and outline the proof below, as the ideas introduced will be useful in proving Propositions 4.3, 4.5, and 4.8 appearing in this section.

Definition 4.1. [BK22b] A diagram D is *homologically A-adequate* if, for any state S with exactly one B-resolution, we have $k(S) \leq k(S_A)$. A diagram D is *homologically B-adequate* if, for any state S with exactly one A-resolution, we have $k(S) \leq k(S_B)$. A diagram D is called *homologically adequate* if it is both homologically A-adequate and homologically B-adequate.

Proposition 4.2. *[BK22b, Proposition 2.8] Reduced alternating diagrams are homologically adequate.*

Proof. Let D be a reduced alternating projection of a link L onto a closed, orientable surface Σ, and let S' be a state with exactly one A-resolution. A surgery from a state S to S' is one of the following three types:

(a) a *merge*, where the total number of loops is reduced- in this case either $k(S') = k(S) - 1$ and $r(S') = r(S)$, or $k(S') = k(S)$ and $r(S') = r(S) - 1$.

(b) a *split*, where the total number of loops is increased- in this case either $k(S') = k(S) + 1$ and $r(S') = r(S)$, or $k(S') = k(S)$ and $r(S') = r(S) + 1$.

(c) a *single cycle smoothing* (defined in [BK22b, Section 2]), where the total number of loops remains the same- in this case $k(S') = k(S)$ and $r(S') = r(S)$.

The key difference between the surface case and the planar case in [DL06] and [Sto06] is the possibility that the kernel is preserved between states, as well as the potential for single cycle smoothings. However, as the authors of [BK22b] point out, single cycle smoothings cannot occur for checkerboard colorable diagrams. Also since every loop in S_A is trivial, any merge would reduce the kernel. The only remaining possibility for the first surgery is a split.

A split occurs when one surgers along an arc in S_A running between a loop and itself. This arc corresponds to a simple closed curve γ in $\mathbb{G}_A$ intersecting D at a single crossing. By the definition of reduced, γ must be homologically essential, otherwise the crossing would be nugatory. Again, since the loops in S_A are trivial, it follows that the new loop resulting from the split is homologous to $\gamma \subset \Sigma$. Thus, $k(S') = k(S_A) - 1$ and $r(S') = r(S_A) + 1 = 1$. The proof for B-adequacy is completely symmetrical. □

In [BK22b, Lemma 2.6] it is shown that for homologically adequate diagrams, S_A and S_B are the unique states which contribute maximal and minimal degree terms of $\langle D \rangle_{\Sigma}^{H}$. We adapt this result to $\langle D \rangle_{\Sigma}$ and restate it in terms of the leading coefficients.

Proposition 4.3. *[BK22b, Lemma 2.6] Let D be a homologically adequate diagram on a closed, orientable surface Σ. Then $\langle D \rangle_{\Sigma}$ has unique terms of maximal and minimal degree in the variable A of the form*

$$(-1)^{v_A} A^{c(D)+2v_A}, \tag{18}$$

$$(-1)^{v_B} A^{-c(D)-2v_B}. \tag{19}$$

Proof. Let S be any state with at least one B-resolution. Suppose $\beta(S) = n \geq 1$ and let $e_1, \cdots, e_n$ be the edges of $\mathbb{G}_A$ that correspond to B-resolved crossings in S, ordered arbitrarily. Surgering along the edges one at a time produces a sequence of states $S_A = S_0, S_1, \cdots, S_n = S$. By homological adequacy, $k(S_1) \leq k(S_0)$. Even if all of the remaining surgeries increase the kernel, we will have $k(S) \leq k(S_0) + (n-1)$. Since S contributes

$$\langle D \mid S \rangle_\Sigma = A^{c(D)-2n}(-A^2 - A^{-2})^{k(S)} Z^{r(S)} W^{\bar{c}(S)}, \tag{20}$$

we have

$$\begin{aligned} \deg^A_{\max}(\langle D \mid S \rangle_\Sigma) &= c(D) - 2n + 2k(S) \\ &\leq c(D) - 2n + 2(k(S_0) + n - 1) \\ &= c(D) + 2v_A - 2. \end{aligned} \tag{21}$$

Therefore, only S_A will contribute a term of A-degree $c(D) + 2v_A$. This term appears in (14), and the proof for the minimal degree term is similar. □

This proposition directly corresponds to the classical results of Kauffman [Kau87], Thistlethwaite [Thi87], and Murasugi [Mur87] which led to a proof of the first and second Tait conjectures using the Jones polynomial. The main purpose of [BK22b] was to extend these results to the setting of homologically adequate links in thickened surfaces.

In the classical planar case, Dasbach and Lin in [DL06] as well as Stoimenow in [Sto06] compute more coefficients. These coefficients have more complicated expressions in terms of data coming from the graphs $\mathbb{G}_A$ and $\mathbb{G}_B$. We will extend their work to

links in surfaces using the more general homological Kauffman bracket. First, we set some terminology. Typically, the term "loop" is used for an edge of a graph which is incident to only one vertex. Since we will be using the word "loop" to refer to the simple closed curves in a state, we will instead call such an edge a *self-edge*. An edge which is incident to two distinct vertices is called a *simple edge*.

Definition 4.4. Let e be a self-edge in either $\mathbb{G}_A$ or $\mathbb{G}_B$. We may view e as a well-defined element $[e]$ of $H_1(\Sigma)$ up to a choice of orientation. We define an equivalence relation $\sim^*$ on self-edges, where $e_1 \sim^* e_2$ if $[e_1] = \pm[e_2]$ and if they are adjacent, meaning incident to the same vertex.

Similarly, let e_1 and e_2 be simple edges in either $\mathbb{G}_A$ or $\mathbb{G}_B$ which are incident to the same pair of vertices. The edges e_1 and e_2 form a cycle in the graph which may also be viewed as an element of $H_1(\Sigma)$ up to orientation. We define an equivalence relation $\sim$ on simple edges, where $e_1 \sim e_2$ if they form a null-homologous cycle.

Let e_A^* and e_B^* denote the number of distinct equivalence classes of self-edges in $\mathbb{G}_A$ and $\mathbb{G}_B$, and let $\tilde{e}_A$ and $\tilde{e}_B$ be the number of distinct equivalence classes of simple edges in $\mathbb{G}_A$ and $\mathbb{G}_B$, respectively.

Proposition 4.5. *Let D be a reduced alternating diagram on a closed, orientable surface Σ. Then, the terms of $\langle D \rangle_\Sigma$ having the second-highest degree in the A variable are of the form*

$$(-1)^{v_A} \ (\alpha'_{(1)} W + \alpha'_{(2)} W^2 + \cdots + \alpha'_{(N)} W^N) \ Z \ A^{c(D)+2v_A-2}, \tag{22}$$

where

$$\alpha'_{(1)} = e_A^*, \tag{23}$$

and the terms having the second-lowest degree are of the form

$$(-1)^{v_B}\ (\beta'_{(1)}W + \beta'_{(2)}W^2 + \cdots + \beta'_{(M)}W^M)\ Z\ A^{-c(D)-2v_B+2}, \tag{24}$$

where

$$\beta'_{(1)} = e^*_B, \tag{25}$$

for some N, $M \geq 1$.

Proof. We look first at all states which contribute to the second-highest A-degree, ignoring Z- and W-degrees for a moment. We should note here that in the binomial expansion of $(-A^2 - A^{-2})^{v_A}$ in $\langle D \mid S_A \rangle_\Sigma$, all degrees of the variable A will be of the form $c(D) + 2v_A - 4k$ for some k, so S_A will not make a contribution. Let $S \in \mathcal{S}$ be any state with $\beta(S) = n \geq 1$, and let $S_A = S_0, S_1, \cdots, S_n = S$ be a sequence of states yielding S as before. By (21), we need to consider states such that $k(S) = k(S_0) + (n-1)$.

Recall that by homological adequacy, $k(S_1) \leq k(S_0)$ but for any other surgery, $k(S_{i+1}) \leq k(S_i) + 1$. In order for $k(S)$ to be maximal, these must all be equalities, in which case the corresponding degree in the A variable will be $c(D) + 2v_A - 2$. We will see that such states have homological rank one, thus proving (22).

We now turn our attention to $\alpha'_{(1)}$, so assume further that $\bar{c}(S) = 1$. Our goal is to understand to what types of surgeries the edges $e_1, \cdots, e_n$ correspond. Recall from the proof of Proposition 4.2 that if the first surgery is to preserve the kernel, then it must be a split. This means that e_1 is a self-edge for a loop l and that surgering l along e_1 produces parallel loops l_1 and l_2 in S_1 which are both homologous to e_1. Thus, $\bar{c}(S_1) = 1$. Note that if there is no such sequence, i.e., if $r(S) = 0$ for all states

S adjacent to S_0, then there are no self-edges. Hence, $\alpha'_{(1)} = e^*_A = 0$ and we are done. Otherwise, each remaining surgery in such a sequence must be a split where $k(S_{i+1}) = k(S_i) + 1$, $r(S_{i+1}) = r(S_i)$, and $\bar{c}(S_{i+1}) = \bar{c}(S_i)$.

Next, we will show by induction that the remaining edges are in the same equivalence class as e_1. Suppose that for all $j \leq i$, e_j is adjacent to e_1 and $i_*(H_1(S_j)) = i_*(H_1(S_1)) = \langle e_1 \rangle \subset H_1(\Sigma)$. Let l' be the loop in S_i corresponding to the vertex incident to e_{i+1}. There are two possibilities.

Case 1 Suppose l' is null-homologous. Because $r(S_{i+1}) = r(S_i) = 1$ and $\bar{c}(S_{i+1}) = \bar{c}(S_i)$, surgering l' along e_{i+1} must produce two homologically trivial loops, as opposed to two parallel essential loops. Note that this would violate homological adequacy if l' had been a loop originating in S_0, since changing the order of edge surgeries so that e_{i+1} is done first would increase the kernel. Thus, l' must have been created by a previous surgery, so e_{i+1} must have been adjacent to e_j for some $j \leq i$. Therefore, $i_*(H_1(S_{i+1})) = \langle e_1 \rangle \subset H_1(\Sigma)$ and the inductive step holds.

Case 2 Suppose $[l'] = [e_1]$. Since $\bar{c}(S_i) = \bar{c}(S_1) = 1$, S_i has two essential loops, one of which is l'. Thus, e_{i+1} must have been adjacent to e_j for some $j \leq i$. Furthermore, the other essential loop homologous to e_1 is unaffected by the surgery. Since $r(S_{i+1}) = r(S_i) = 1$, surgering l' along e_{i+1} must produce one null-homologous loop and one loop homologous to e_1. This gives $i_*(H_1(S_{i+1})) = i_*(H_1(S_i)) = \langle e_1 \rangle$ and thus, the inductive step holds.

Therefore, $i_*(H_1(S)) = \langle e_1 \rangle \subset H_1(\Sigma)$ and all the edges are adjacent to e_1. Changing the order of edge surgeries so that e_i is done first will still yield the same state S, implying $[e_i] = [e_1]$ for all i. This means precisely that $e_i \sim^* e_1$ for all i.

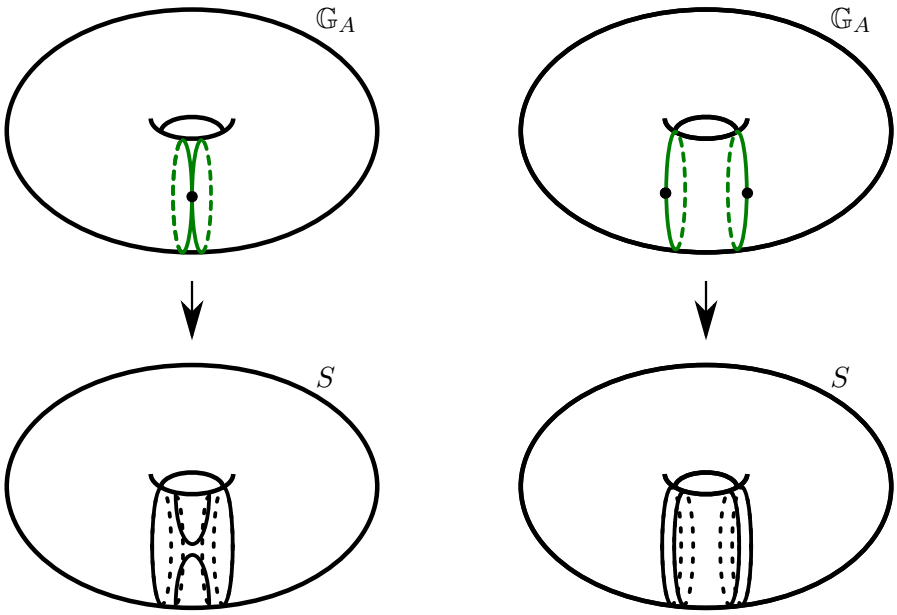

Figure 12: Left: Surgering along self-edges in the same equivalence class. Right: Surgering along merely homologous self-edges.

Let S be a state whose B-resolutions occur within a single equivalence class of self-edges. Let e_i^A be the i-th of these classes, and let k_i be the number of self-edges in that class. The total contribution of these states is

$$\begin{aligned}
&\sum_{i=1}^{e_A^*}\sum_{j=1}^{k_i}\binom{k_i}{j}A^{c(D)-2j}(-A^2-A^{-2})^{v_A+j-1}ZW \\
&\quad=\sum_{i=1}^{e_A^*}\sum_{j=1}^{k_i}\binom{k_i}{j}A^{c(D)-2j}(-1)^{v_A+j-1}(A^2+A^{-2})^{v_A+j-1}ZW \\
&\quad=\sum_{i=1}^{e_A^*}\sum_{j=1}^{k_i}\binom{k_i}{j}A^{c(D)-2j}(-1)^{v_A+j-1}(A^{2v_A+2j-2}+\text{lower-order terms})ZW \\
&\quad=\sum_{i=1}^{e_A^*}\sum_{j=1}^{k_i}\binom{k_i}{j}(-1)^{v_A+j-1}A^{c(D)+2v_A-2}ZW+\text{lower-order terms} \\
&\quad=\sum_{i=1}^{e_A^*}(-1)^{v_A}A^{c(D)+2v_A-2}ZW+\text{lower-order terms} \\
&\quad=(-1)^{v_A}e_A^*A^{c(D)+2v_A-2}ZW+\text{lower-order terms},
\end{aligned}$$

proving (23). The second-to-last equality follows from the fact that $\sum_{j=0}^{k}(-1)^j\binom{k}{j} = 0$. To compute the coefficient $\beta'_{(1)}$, an analogous argument holds for states whose A-resolutions lie in the same equivalence class of self edges. □

Remark 4.6. In the calculation above, note that in order for $\bar{c}(S)$ to equal one, the self-edges in S must be adjacent. In general, $\bar{c}(S)$ counts the number of vertices which house edges that are homologous, but not equivalent under $\sim^*$. This is illustrated in Figure 12. The numbers N and M in the statement of the proposition are the maximum numbers of these vertices, taken over the set of all homology classes of self-edges.

Since it is possible for a diagram to have no self-edges, we cannot establish a meaningful lower bound for any combination of $\alpha'_{(1)}$ and $\beta'_{(1)}$. It is then necessary to look at more coefficients.

Definition 4.7. Let e_1 and e_2 be adjacent self-edges in either $\mathbb{G}_A$ or $\mathbb{G}_B$ whose homology classes have intersection number $int([e_1],[e_2]) = \pm 1$. We call the unordered double (e_1, e_2) a *transverse pair* of self-edges.

If (e_1, e_2) is a transverse pair, it is possible that there exists a third self-edge e_3 such that $[e_3] = \pm[e_1] \pm [e_2]$. In this case, we call the unordered triple (e_1, e_2, e_3) a *self-triangle*.

The equivalence relation, $\sim^*$, on self-edges also induces equivalence relations on transverse pairs and self-triangles. Let $\pitchfork^*_A$ and $\pitchfork^*_B$ denote the number of equivalence classes of transverse pairs of self-edges, and let τ^*_A and τ^*_B denote the number of equivalence classes of self-triangles in $\mathbb{G}_A$ and $\mathbb{G}_B$, respectively. See Figure 13 for an example of a transverse pair and a self-triangle.

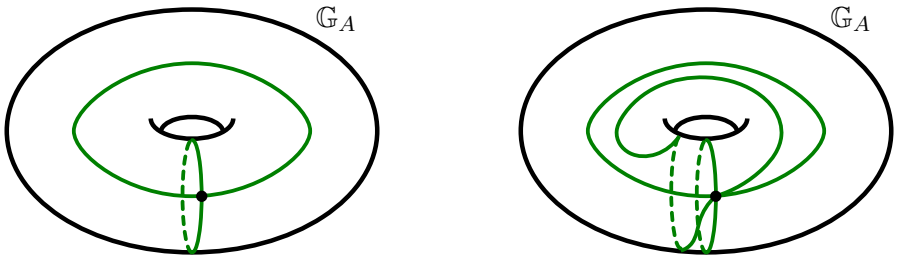

Figure 13: Left: A transverse pair. Right: A self-triangle.

Proposition 4.8. *Let D be a reduced alternating diagram on a closed, orientable surface Σ. Then, the terms of $\langle D\rangle_\Sigma$ having the third-highest degree in the variable A are of the form*

$$(-1)^{v_A}(\alpha''_{(0)} + \alpha''_{(2)}Z^2)A^{c(D)+2v_A-4}, \tag{26}$$

where

$$\alpha''_{(0)} = v_A - \tilde{e}_A + \pitchfork^*_A - \tau^*_A \text{ and } \alpha''_{(2)} = \binom{e^*_A}{2} - \pitchfork^*_A, \tag{27}$$

and the terms having the third-lowest degree in the variable A are of the form

$$(-1)^{v_B}(\beta''_{(0)} + \beta''_{(2)}Z^2)A^{-c(D)-2v_B+4}, \tag{28}$$

where

$$\beta''_{(0)} = v_B - \tilde{e}_B + \pitchfork^*_B - \tau^*_B \text{ and } \beta''_{(2)} = \binom{e^*_B}{2} - \pitchfork^*_B\ . \tag{29}$$

Note that these coefficients contain elements of both second and third coefficients from the planar case in [DL06] and [Sto06]. The reason for this is the possibility for the kernel to be preserved at the first surgery, whereas in the planar case the number of loops can only decrease at the first surgery. For the first surgery, only self-edges preserve the kernel, which is why the terms for self-triangles and pairs of self-edges appear here, while corresponding terms for simple edges do not.

Proof. By (20), the third-highest possible degree of $\langle D \rangle_\Sigma$ in the variable A is $c(D) + 2v_A - 4$. Notice that this time, S_A will make a contribution. We get

$$\begin{aligned}\langle D \mid S_A \rangle_\Sigma &= A^{c(D)}(-A^2 - A^{-2})^{v_A} \\ &= (-1)^{v_A} A^{c(D)}(\text{higher-order terms} + v_A A^{2v_A - 4} + \text{lower-order terms}) \\ &= \text{higher-order terms} + (-1)^{v_A} v_A A^{c(D)+2v_A-4} + \text{lower-order terms}.\end{aligned}$$

On the other hand, states of the form described in the previous proposition will not contribute anything (the degrees of A in the binomial expansion are of the wrong form: $c(D) + 2v_A - 2 - 4k$, for some k).

Now suppose that S is a state with $\deg_{\max}(\langle D \mid S \rangle_\Sigma) = c(D) + 2v_A - 4$. As in the proof of the previous proposition, let $e_1, \cdots, e_n$ be a sequence of edges of $\mathbb{G}_A$, and $S_A = S_0, S_1, \cdots, S_n = S$ the sequence of states obtained by surgering along each edge in order. As before, we seek to determine which types of surgeries could have yielded S. By homological adequacy, $k(S_1) \leq k(S_0)$. There are two cases, depending on whether the first surgery reduces the kernel or preserves the kernel.

Case 1 If $k(S_1) = k(S_0) - 1$, then e_1 is a simple edge, whose surgery merges two trivial loops l_1 and l_2 in S_0 into a single trivial loop l'. Then $r(S_1) = 0$. In order for the remaining surgeries to yield the desired degree of A, they must all be splits which increase the kernel. In particular, e_2 must split a trivial loop in S_1 into two null-homologous loops. By homological adequacy, this initial loop must be l' and furthermore, in $\mathbb{G}_A$, e_2 must have been a simple edge connecting the same two vertices as e_1. It follows that e_1 and e_2 must have formed a null-homologous curve. This means precisely that $e_1 \sim e_2$. By reordering the sequence of edges we see that $e_i \sim e_1$ for all $2 \leq i \leq n$.

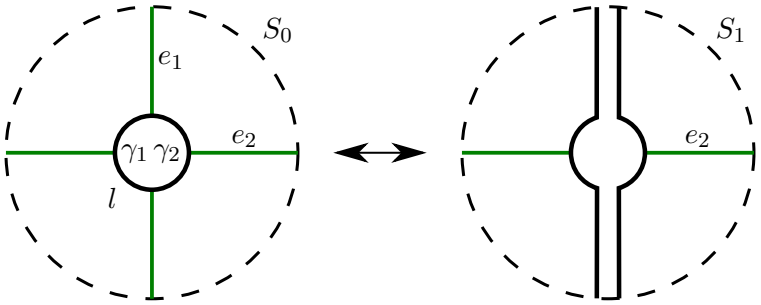

Figure 14: A state in case 2a.

The total contribution of states whose B-resolutions occur within a single equivalence class of simple edges is

$$\sum_{i=1}^{\tilde{e}_A}\sum_{j=1}^{k_i}\binom{k_i}{j}A^{c(D)-2j}(-A^2-A^{-2})^{v_A+j-2}$$
$$= (-1)^{v_A-1}\tilde{e}_A A^{c(D)+2v_A-4} + \text{lower-order terms},$$

where the equality follows from the same steps used in the proof of Proposition 4.5.

Case 2 If $k(S_1) = k(S_0)$ then e_1 was a self-edge as in the proof of the previous proposition, and $r(S_1) = 1$. In order for the state S to contribute to the desired degree of A, there must be a $j, 1 < j \leq n$ such that $k(S_j) = k(S_{j-1})$, and for all $i \neq 1, j$ we have $k(S_i) = k(S_{i-1}) + 1$ while the homological rank is preserved. Note that the j-th surgery could either be a merge resulting in $r(S_n) = r(S_j) = 0$ or a split resulting in $r(S_n) = r(S_j) = 2$. First, let us deal with the scenario that the j-th surgery is a merge.

Case 2a We first claim that in such a scenario, all of the edges had to be adjacent self-edges. Indeed, the proof of the previous proposition implies that e_i for $1 \leq i < j$ are all homologous and that $H_1(S_i) = \langle e_1 \rangle$ (but we cannot yet conclude they are adjacent). However, since $r(S_j)$ must be zero, surgery along e_j must be a merge

which reduces the homological rank. This is only possible if S_{j-1} contains exactly two essential loops l_1 and l_2, making $\bar{c}(S_{j-1}) = 1$. We saw that this can only happen if the e_i are adjacent, and therefore belong to the same equivalence class for $1 \leq i < j$. Surgery along e_j merges l_1 and l_2 into a single null-homologous loop l', so e_j must have been adjacent to e_i for some $i < j$. At this point, all loops in S_j are null-homologous, so the remaining surgeries must split off more null-homologous loops. By a similar homological adequacy argument as in the proof of the previous proposition, e_i for $j < i \leq n$ also must be adjacent to the previous edges.

Now that we know all edges in such a state must be incident to a single vertex v in $\mathbb{G}$, it will suffice to look at a local neighborhood of the loop l in S_A corresponding to v. Without loss of generality, assume that $j = 2$. As seen in Figure 14, e_1 splits l into two arcs, γ_1 and γ_2 which correspond to the loops l_1 and l_2. Since surgery along e_2 merges l_1 and l_2, it must connect γ_1 and γ_2 outside of the disk region bounded by l. (This can only happen if $g(\Sigma) > 0$.) In this way, we see that e_1 and e_2 are transverse.

Now, let us address the edges e_i, $2 < i \leq n$ whose surgeries increase the kernel. As seen in Figure 15, e_1 and e_2 divide l into four arcs, γ_k, $k = I, II, III, IV$. The loop $l' \in S_2$ is a boundary component of a regular neighborhood of $l \cup e_1 \cup e_2$, which may be viewed as the union of corresponding arcs γ'_k and two parallel copies of each of the edges e_1 and e_2. Consider e_3. By homological adequacy, the endpoints of e_3 must lie in different arcs. This leaves us with two possibilities.

Case 2a(i) Suppose that e_3 connects two adjacent arcs. Since $k(S_3) = k(S_2) + 1$, surgery along e_3 splits off a null-homologous loop from l'. In other words, e_3 along with an arc in l' forms a null-homologous loop, independent of the choice of arc. As seen in Figure 15, this arc may be taken to be one of the edges e_i, $i = 1, 2$. Thus, $e_3 \sim^* e_i$. If all remaining e_i, $3 \leq i \leq n$ behave this way, then S is a state whose

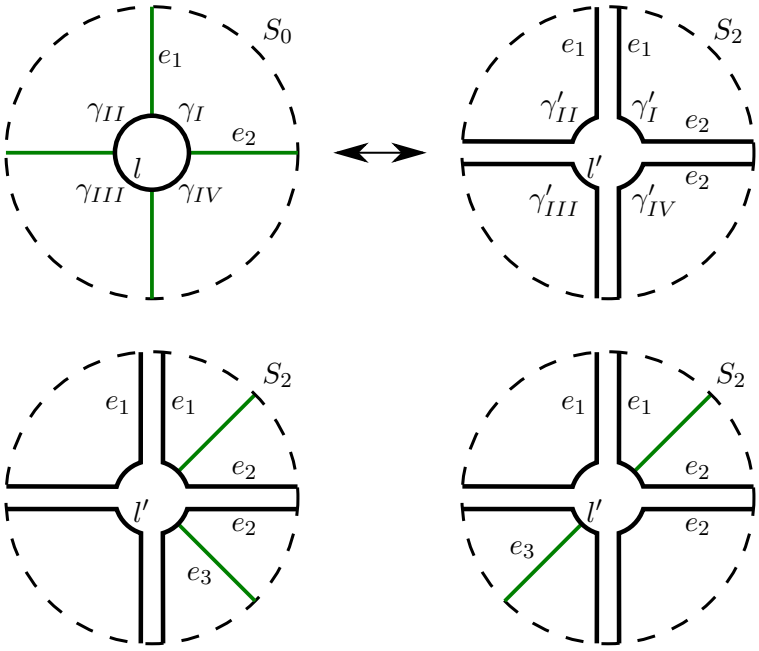

Figure 15: Bottom left: A state in case 2a(i). Bottom right: A state in case 2a(ii).

B-resolutions appear within a single equivalence class of the transverse pair (e_1, e_2), which we denote by $(e_1, e_2)^*$. The total contribution of such states is

$$\sum_{(e_1,e_2)^*} \sum_{i=1}^{k_{e_1}} \sum_{j=1}^{k_{e_2}} \binom{k_{e_1}}{i} \binom{k_{e_2}}{j} A^{c(D)-2(i+j)} (-A^2 - A^{-2})^{v_A+i+j-2}$$

$$= (-1)^{v_A} \Cap_A^* \, A^{c(D)+2v_A-4} + \text{lower-order terms},$$

where k_{e_1} and k_{e_2} denote the number of edges in the equivalence classes of e_1 and e_2, respectively.

Case 2a(ii) Suppose that e_3 connects two opposite arcs. This time, the arc in l' is a combination of e_1 and e_2. This means precisely $[e_3] = \pm[e_1] \pm [e_2] \in H_1(\Sigma)$. Thus (e_1, e_2, e_3) is a self-triangle. Note that if such an e_3 exists, no edge can connect the other pair of opposite γ_k in l. Otherwise, if there did exist such an edge e', consider the intersection number $int(e', e_3) = int(e', e_1) + int(e', e_2)$. Since $\mathbb{G}_A$ is embedded

in Σ, we would have $int(e', e_1) = int(e', e_2) = int(e', e_1) + int(e', e_2) = \pm 1$ which is impossible. Therefore, for $3 < i \leq n$ e_i falls under case 2a(i) or 2a(ii) and as such belongs to the equivalence class of either e_1, e_2, or e_3. Then S is a state whose B-resolutions appear within a single equivalence class of the self-triangle (e_1, e_2, e_3), which we denote by $(e_1, e_2, e_3)^*$. The total contribution of such states is

$$\sum_{(e_1,e_2,e_3)^*} \sum_{i=1}^{k_{e_1}} \sum_{j=1}^{k_{e_2}} \sum_{k=1}^{k_{e_3}} \binom{k_{e_1}}{i} \binom{k_{e_2}}{j} \binom{k_{e_3}}{k} A^{c(D)-2(i+j+k)} (-A^2 - A^{-2})^{v_A+i+j+k-2}$$
$$= (-1)^{v_A-1} \tau_A^* A^{c(D)+2v_A-4} + \text{lower-order terms}$$

Case 2b Lastly, we address the other scenario described at the beginning of case 2, where the j-th surgery is a split which increases the homological rank rather than the kernel. The only possibility left is that e_j is a self-edge which is neither transverse nor homologous to e_1. Once again, all other edges must belong to the equivalence class of either e_1 or e_j. Letting e_1^* and e_2^* denote the two classes, the total contribution of these states is

$$\sum_{\substack{e_1^* \neq e_2^* \\ \text{not transverse}}} \sum_{i=1}^{k_{e_1}} \sum_{j=1}^{k_{e_2}} \binom{k_{e_1}}{i} \binom{k_{e_2}}{j} A^{c(D)-2(i+j)} (-A^2 - A^{-2})^{v_A+i+j-2} Z^2$$
$$= (-1)^{v_A} \left(\binom{e_A^*}{2} - \pitchfork_A^* \right) A^{c(D)+2v_A-4} Z^2 + \text{lower-order terms}$$

Combining the contributions from S_A, case 1, and case 2a, we get $\alpha''_{(0)} = v_A - \tilde{e}_A + \pitchfork_A^* - \tau_A^*$ as claimed. Likewise, case 2b gives $\alpha''_{(2)} = \binom{e_A^*}{2} - \pitchfork_A^*$. An analogous argument holds for $\beta''_{(0)}$ and $\beta''_{(2)}$. □

4.2 Bounds on the twist number

The goal of this section is to prove Main Theorem 1. Let $e'_A = e^*_A + \tilde{e}_A$ and $e'_B = e^*_B + \tilde{e}_B$. We consider the quantity

$$\begin{aligned} \star &= \alpha'_{(1)} + \beta'_{(1)} - \alpha''_{(0)} - \beta''_{(0)} + 2 \\ &= e'_A + e'_B - v_A - v_B + 2 + \tau^*_A + \tau^*_B - \Cap^*_A - \Cap^*_B \, . \end{aligned} \tag{30}$$

We now seek to bound $\star$ in terms of the twist number of the diagram. We follow the method used for the planar case in [FKP08]. As transverse edge pairs (and by extension self-triangles) do not arise in the planar case, we deal with these terms first.

Proposition 4.9. *Suppose Σ has genus g. Then,*

$$-2g \leq \tau^*_A + \tau^*_B - \Cap^*_A - \Cap^*_B \leq 0. \tag{31}$$

Proof. The second inequality is immediate from the fact that every self-triangle consists of three self-edges which are all pairwise transverse. Furthermore, no pair can be part of any other self-triangle since the third self-edge is already determined by the pair.

For the first inequality, we will show that $\tau^*_A + \tau^*_B \leq g$. Suppose without loss of generality that $\mathbb{G}_A$ contains a self-triangle class $(e_1, e_2, e_3)^*$ at a vertex corresponding to the loop l. Figure 16 shows the result of surgering l along e_1, e_2, and e_3 to obtain the state S, where e'_1, e'_2, and e'_3 are the surgery arcs dual to these edges. In place of the self-triangle, there is a region R which is a punctured torus. Note that $\Sigma \setminus R$ then consists of two punctured surfaces with total genus $g - 1$. Iterating this argument, we immediately see that $\mathbb{G}_A$ can have at most g self-triangle classes.

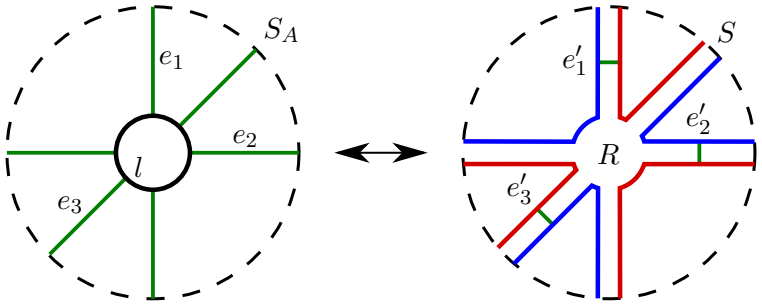

Figure 16: The result of surgering along a self-triangle. The red and blue loops bound separate punctured surfaces.

More is true, however. Notice that e'_1, e'_2, and e'_3 are the only surgery arcs joining these punctured surfaces. Thus, when we complete the remaining surgeries to obtain S_B, the arcs e'_1, e'_2, and e'_3 become identified with simple edges of $\mathbb{G}_B$. By reordering, this will also be the case for the other edges making up $(e_1, e_2, e_3)^*$. Therefore, the remaining surgeries induce an isotopy on R taking it to a punctured torus in Σ which contains no self-edges of $\mathbb{G}_B$. We have shown that the presence of a self-triangle class in either $\mathbb{G}_A$ or $\mathbb{G}_B$ obstructs the existence of a potential set of transverse self-edge classes (and by extension a self-triangle) in the other. Iterating this argument, we have $\tau^*_A + \tau^*_B \leq g$ as claimed.

Recall that across both state graphs, there are a total of $3(\tau^*_A + \tau^*_B)$ classes of transverse pairs coming from self-triangles. By an analogous argument, in $\mathbb{G}_A$ there are at most $g - (\tau^*_A + \tau^*_B)$ pairs which are not part of any self-triangle. By contrast, these do not obstruct a transverse pair in $\mathbb{G}_B$: for an example, see the left-hand graph depicted in Figure 13 and note that it is isotopic to its dual.

Therefore, the same bound holds for $\mathbb{G}_B$. By adding across both state graphs, we have

$$\begin{aligned} \curlywedge^*_A + \curlywedge^*_B &\leq 3(\tau^*_A + \tau^*_B) + 2g - 2(\tau^*_A + \tau^*_B) \\ &= 2g + \tau^*_A + \tau^*_B. \end{aligned} \tag{32}$$

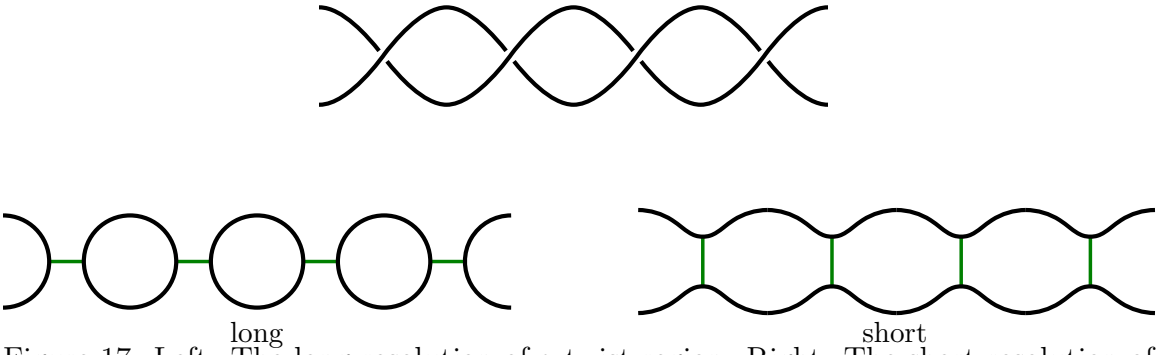

Figure 17: Left: The long resolution of a twist region. Right: The short resolution of a twist region.

This implies

$$\tau_A^* + \tau_B^* - \Cap_A^* - \Cap_B^* \geq -2g, \tag{33}$$

as desired. □

In [FKP08], the authors bound the quantity analogous to $\star$ from above by recategorizing the vertices and edges based on how twist regions in D reveal themselves in two different ways in each of the state graphs.

Definition 4.10. Referring to Figure 17, we call these *long* and *short* resolutions. Edges are also called *long* and *short* if they come from that type of resolution. Let e'_{long} denote the number of equivalence classes of long edges across both $\mathbb{G}_A$ and $\mathbb{G}_B$, and let e'_{short} denote the number of equivalence classes of short edges across both graphs.

Notice that short edges coming from the same twist region are all in the same equivalence class. This is the exact same property exhibited by the "reduced edges" in [FKP08] which leads to Proposition 4.6, the upper bound in the planar case. We adapt this proposition and its proof to the current setting.

Proposition 4.11. *[FKP08, Proposition 4.6] Let D be a reduced alternating diagram on a closed, orientable surface Σ. Then,*

$$e'_A + e'_B - v_A - v_B + 2 \leq 2\ tw(D). \tag{34}$$

Proof. Let v_{bigon} denote the number of bigon vertices across both $\mathbb{G}_A$ and $\mathbb{G}_B$. Bigon vertices are incident to exactly two edges and correspond to the vertices in the long resolution of a twist region. Let $v_{\text{n-gon}}$ to be the total number of remaining vertices. Every vertex and edge across both state graphs falls into exactly one of two categories, so we can regroup $e'_A + e'_B - v_A - v_B = e'_{\text{short}} + e'_{\text{long}} - v_{\text{bigon}} - v_{\text{n-gon}}$.

For R a twist region, write $c(R)$ for the number of crossings in R. Notice that R consists of $c(R) - 1$ bigon regions. Adding across all twist regions, we obtain $v_{\text{bigon}} = c(D) - t(D)$. Next observe that, except for $(2, q)$-torus link diagrams on S^2, both $\mathbb{G}_A$ and $\mathbb{G}_B$ will contain at least one n-gon vertex, making $v_{\text{n-gon}} \geq 2$. However, (34) can still be seen to hold for $(2, q)$-torus link diagrams, which have $t(D) = 1$.

From the earlier observation that the edges in a short resolution are equivalent, we have $e'_{\text{short}} \leq t(D)$. Additionally, each crossing can have at most one long resolution, so $e'_{\text{long}} \leq c(D)$. We have

$$\begin{aligned} e'_{\text{short}} + e'_{\text{long}} - v_{\text{bigon}} - v_{\text{n-gon}} &\leq t(D) + c(D) - (c(D) - t(D)) - 2 + 2 \\ &= 2t(D), \end{aligned}$$

as desired. □

For the lower bound, only a slight modification of the methods used in the planar case is required. Let us first summarize the argument, which appears in Section 4.3 of [FKP08]. The authors first assume that there are no single-crossing twist regions, so that each region contains at least one bigon. Recall that D may be viewed as a 4-valent graph Γ. They obtain a new 3-valent graph P by collapsing strings of bigons in Γ to red edges. A 2-valent graph, Φ may be obtained by deleting the red edges. Figure 18 depicts these graphs.

The authors call the regions of P "provinces" and the regions of Φ "countries." In [FKP08], the graphs are all constructed on the Turaev surface of D, but since we only deal with alternating links, the graphs P and Φ embed naturally on Σ. Note that P inherits the cellular embedding of D, so all provinces are disks, while countries may be nontrivial regions. For each country, its provinces correspond to n-gon vertices of either $\mathbb{G}_A$ or $\mathbb{G}_B$. The red edges which divide countries into provinces are dual to sets of parallel short edges which connect the two provinces. Recall that if short edges are dual to the same red edge, then they are in the same equivalence class. The converse is not true, however; there may exist short edges dual to distinct red edges which will become identified. The key to the authors' argument is to realize that these different short edges must lie in the same country. So, to find a lower bound the authors investigate the number of short edges in each country that will survive when we pass to equivalence classes. We now prove an analogue of their result [FKP08, Lemma 4.8].

Figure 18: The graphs Γ, P, and Φ.

Proposition 4.12. *Let D be a reduced alternating diagram on a closed, orientable surface Σ such that every twist region of D has at least two crossings. Let N be a country of D, and let $e'_{short}(N)$ denote the number of equivalence classes of short edges contained in N and $e^*_\partial(N)$ the number of self-edge equivalence classes in N which are homologous to a boundary component of N. Let $tw(N)$ denote the number of twist regions in N and let $|\partial N|$ denote the number of loops in Φ which bound N. Then we have*

$$e'_{short}(N) \geq tw(N) + 1 - |\partial N| + e^*_\partial(N). \tag{35}$$

Proof. Consider the dual graph of N, defined to be a connected ribbon graph G whose vertices are the provinces of N, edges are dual to the red edges in N, and boundary components are the loops in Φ which bound N. In [FKP08], the authors obtain a lower bound by finding a spanning tree of G, or alternatively by cutting N along red edges until a disk remains. In our case, it suffices to do the same with a spanning quasi-tree of G.

A *quasi-tree* is a ribbon graph with exactly one boundary component. We can obtain a spanning quasi-tree by removing edges as long as they reduce the number of boundary components of the graph, which corresponds to cutting N along dual red edges. Thus, it suffices to cut N along $|\partial N| - 1$ red edges.

Note that if G is a quasi-tree, then N cannot contain any short edges which are in the same equivalence class, yet are dual to different red edges. Otherwise, these short edges form a null-homologous curve separating N, forcing there to be at least two

boundary components. Also note that there can be no self-edges which are homologous to a boundary component of N for the exact same reason. Recall that a cellularly embedded diagram must be connected, so that all self-edges are short.

Thus, any classes we are left with correspond to a unique one of the remaining $tw(N) + 1 - |\partial N|$ red edges left in the country. Adding back in the self-edge classes which were removed, we obtain the desired inequality. □

The final step in [FKP08] is to find a bound on the number of countries. A small but important modification is needed here. In the planar case, the authors show that every component of Φ contains at least three vertices. As we will see, this does not hold in the surface case, and this issue must be resolved in order to avoid canceling the term for the twist number in the lower bound.

Proposition 4.13. *Let D be a reduced alternating diagram on a closed, orientable surface Σ such that every twist region of D has at least two crossings. Then,*

$$e'_{short} \geq \frac{1}{3} tw(D) + 1 - g(\Sigma). \tag{36}$$

Proof. Let ϕ be a component of Φ which may be thought of as a simple closed curve in Σ. Since D is reduced, ϕ must contain at least two vertices, or else it would bound a monogon region corresponding to a nugatory crossing. We call ϕ "bad" if it has exactly two vertices and "good" if it has at least three. Let $|\Phi|_{\text{bad}}$ denote the number of bad curves and $|\Phi|_{\text{good}}$ the number of good curves, and $|\Phi|$ the total number of curves.

Suppose ϕ is bad. Then because P is cellularly embedded, the two red edges incident to the vertices of ϕ must lie on opposite sides of ϕ. Otherwise, ϕ would bound a bigon region, and all bigons were collapsed in the construction of P. Also note that

Φ inherits the checkerboard coloring of D, so we see that these are indeed distinct red edges which lie in separate countries. By following along ϕ, we see that on each side of ϕ the red edge forms a border between a province and itself. Thus, the red edge is dual to a self-edge which represents the same homology class as ϕ in $H_1(\Sigma)$. This is illustrated in Figure 19. By homological adequacy, we have that this self-edge along with ϕ are homologically essential. In a country N, there can be at most two essential boundary components which are homologous. To see this, recall that these two homologous curves separate Σ, so a third one would separate N. Therefore, for each bad curve there are two boundary-homologous classes of self-edges in the neighboring countries, and there is at worst a 2:1 correspondence between bad curves and a given self-edge class. Therefore, $e^*_\partial \geq |\Phi|_{\text{bad}}$ where $e^*_\partial = \sum_N e^*_\partial(N)$.

The total number of vertices in P is at least three times the number of good edges. Since every red edge has two vertices, this gives us that $tw(D) \geq \frac{3}{2}|\Phi|_{\text{good}}$. Let $n(D)$ denote the number of countries in Φ. By summing (35) over all countries, we get

$$\begin{aligned} e'_{\text{short}} &\geq tw(D) + n(D) - 2|\Phi| + e^*_\partial \\ &\geq tw(D) + n(D) - 2|\Phi| + |\Phi|_{\text{bad}} \\ &= tw(D) + n(D) - |\Phi| - |\Phi|_{\text{good}} \\ &\geq \frac{1}{3}tw(D) + n(D) - |\Phi| \\ &\geq \frac{1}{3}tw(D) + 1 - g(\Sigma). \end{aligned}$$

□

The last inequality follows from the fact that if we cut Σ along the simple closed curves in Φ, at most g of these cuts are non-separating.

We combine these results into a proposition mirroring [FKP08, Theorem 4.10].

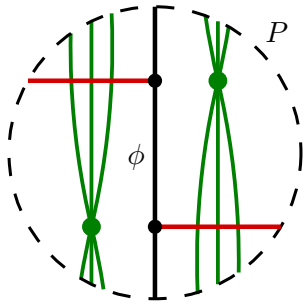

Figure 19: A bad loop. The boundary-homologous self-edges are drawn in green.

Proposition 4.14. *Let D be a reduced alternating diagram on a closed, orientable surface Σ such that every twist region of D has at least three crossings. Then,*

$$\star \geq \frac{1}{3}tw(D) + 1 - g(\Sigma). \tag{37}$$

Proof. When every twist region has at least three crossings, no two long edges can be in the same equivalence class. By summing over every twist region as in the proof of Proposition 4.11, we see that $v_{\text{bigon}} = c(D) - t(D)$ and $e'_{\text{long}} = c(D)$. Recall that the n-gon vertices become provinces in P, and the twist regions become red edges. Therefore, by summing over countries, we can compute $\chi(\Sigma) = v_{\text{n-gon}} - tw(D)$. Putting this all together,

$$\begin{aligned}
\star &= e'_A + e'_B - v_A - v_B + 2 + \tau^*_A + \tau^*_B - \pitchfork^*_A - \pitchfork^*_B \\
&= e'_{\text{short}} + e'_{\text{long}} - v_{\text{bigon}} - v_{\text{n-gon}} + 2 + \tau^*_A + \tau^*_B - \pitchfork^*_A - \pitchfork^*_B \\
&= e'_{\text{short}} + c(D) - (c(D) - tw(D)) - v_{\text{n-gon}} + 2 + \tau^*_A + \tau^*_B - \pitchfork^*_A - \pitchfork^*_B \\
&= e'_{\text{short}} - \chi(\Sigma) + 2 + \tau^*_A + \tau^*_B - \pitchfork^*_A - \pitchfork^*_B \\
&\geq e'_{\text{short}} - \chi(\Sigma) + 2 - 2g(\Sigma) \\
&= e'_{\text{short}} \\
&\geq \frac{1}{3}tw(D) + 1 - g(\Sigma).
\end{aligned}$$

□

Combining (34) and (37), we obtain a proof of Theorem 1.

In [KP20], the authors bound the hyperbolic volume of the complement of a "weakly generalized" alternating link in terms of the twist number. A weakly generalized alternating link is a link in a compact, irreducible, orientable 3-manifold with a projection onto a surface Σ with some additional properties that guarantee the complement admits a complete hyperbolic structure. They also require the diagram to be twist-reduced as in Definition 3.11.

Theorem 4.15. *[KP20, Theorem 1.4] Let Σ be a closed orientable surface of genus at least one, and let L be a link that admits a twist-reduced weakly generalized cellularly embedded alternating projection D onto $\Sigma \times \{0\}$ in $Y = \Sigma \times [-1, 1]$. Then the interior of $Y \setminus L$ admits a hyperbolic structure. If Σ is a torus, then we have*

$$\frac{v_{oct}}{2} \cdot tw(D) \leq Vol(Y \setminus L) < 10v_{tet} \cdot tw(D), \tag{38}$$

where $v_{tet} \approx 1.01494$ is the volume of a regular ideal tetrahedron, and $v_{oct} \approx 3.66386$ is the volume of a regular ideal octahedron.

If Σ has genus at least two,

$$\frac{v_{oct}}{2} \cdot (tw(D) - 3\chi(\Sigma)) \leq Vol(Y \setminus L) < 6v_{oct} \cdot tw(D). \tag{39}$$

Direct substitution of (4) into these volume bounds yields Corollary 1.4.

4.3 Discussion of results

The above results first appeared in the author's paper [Wil22]. We should note that while that paper was in preparation, related results were independently obtained for different choices of polynomials. Champanerkar and Kofman [CK22] use the homological Kauffman bracket (see Definition 3.3), while Bavier and Kalfagianni [BK22a] define a polynomial $\langle D \rangle_0$ which agrees with the classical Kauffman bracket, but is defined over states consisting only of contractible loops. In contrast to Theorem 1, both of these results contain strict equalities between coefficients and the twist number, rather than inequalities. There is, however, an associated cost. In [CK22] the authors must use a homological version of the twist number, and in [BK22a] the notion of "reduced" is stronger which eliminates many of the terms making up $\star$ in (30). Although we achieve only inequalities, our approach has the advantage of recovering the classical twist number without requiring these further conditions.

5 Quantum invariants of 3-manifolds

5.1 Skein theory and quantum invariants

Now, let us return to the planar setting where we may discuss the topic of quantum invariants. For a link $L \subset S^3$ we may set $\Sigma = S^2$ in Definition 3.4 to recover the classical Kauffman bracket. For the remainder of the paper, we will change to the variable $q = A^2$. The Kauffman bracket state-sum becomes

$$\langle D \rangle = \sum_{S \in \mathcal{S}} q^{\frac{1}{2}(\alpha(S)-\beta(S))}(-q-q^{-1})^{|S|}, \tag{40}$$

where $|S|$ is the number of loops in the state S. Skein theory, introduced in [Prz91], provides a convenient framework for studying the Kauffman bracket and defining the colored Jones polynomials and related quantum invariants.

Definition 5.1. Let Σ be a compact orientable surface, with or without boundary. If $\partial\Sigma \neq \emptyset$, let $\partial\Sigma$ contain a (possibly empty) finite set of n marked points. The *Kauffman bracket skein module* of Σ, denoted either $\mathcal{S}(\Sigma)$ or $\mathcal{S}(\Sigma, n)$, is defined to be the $\mathbb{Z}[q^{\pm\frac{1}{2}}]$-module consisting of formal linear sums of isotopy classes of link diagrams on Σ under the quotient by the Kauffman relations:

1. $D \sqcup$ (a trivial closed curve) $= (-q-q^{-1})D$,
2. 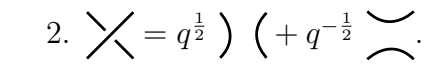 $= q^{\frac{1}{2}}$) ($+ q^{-\frac{1}{2}}$.

When $\partial\Sigma \neq \emptyset$, the link diagrams are assumed to intersect $\partial\Sigma$ at the marked points if $n > 0$.

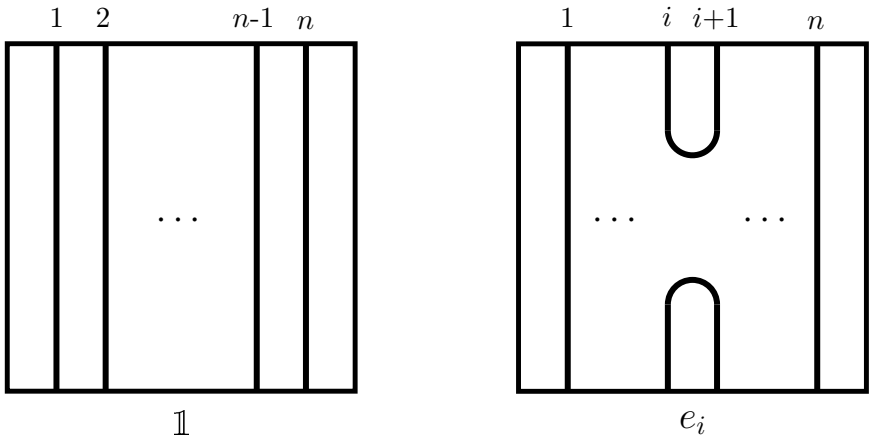

Figure 20: Left: The identity diagram $\mathbb{1}$. Right: The generator e_i, $i = 1 \dots n-1$.

Note that $\mathcal{S}(S^2)$ is one-dimensional, being generated by the empty diagram. The Kauffman relations can be seen to give a recurrence relation that is equivalent to (40). Another skein module of key importance is $\mathcal{S}(D^2, 2n)$, the skein of the disk containing $2n$ marked points on its boundary. The set of crossing-less link diagrams in D^2 forms an (additive) basis for $\mathcal{S}(D^2, 2n)$. The disk is normally depicted as a square with n marked points on the top edge and n on the bottom. This module has a natural multiplicative structure which turns it into an algebra.

Definition 5.2. The *n-th Temperley–Lieb algebra*, TL_n is the algebra over $\mathcal{S}(D^2, 2n)$ with multiplication given by vertical stacking of the square diagrams, extended linearly. A (multiplicative) basis is given by the set of diagrams $\{\mathbb{1}, e_1, \dots, e_{n-1}\}$ depicted in Figure 20. The generators e_i, $i = 1, \dots, n-1$ are commonly called "turn-backs."

Under the vertical stacking operation, the generators satisfy the relations

1. $e_i^2 = (-q - q^{-1})e_i$,

2. $e_i e_j = e_j e_i$ if $|i - j| \geq 2$, and

3. $e_i e_{i\pm1} e_i = e_i$.

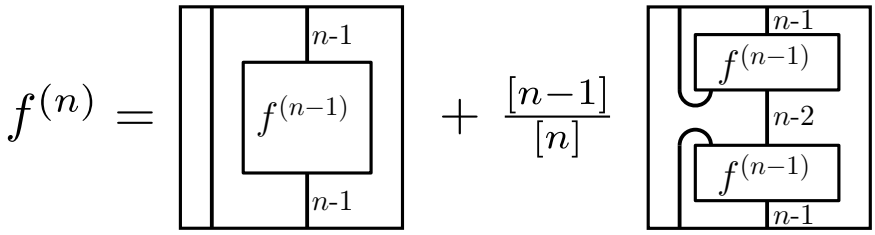

Figure 21: The recursive construction of $f^{(n)}$. A strand labeled by an integer k represents k parallel strands.

A few polynomials in $\mathbb{Z}[q^{\pm\frac{1}{2}}]$ will appear frequently in the coefficients for elements of TL_n in the following sections. They are called *quantum integers* and are defined for $k \in \mathbb{Z}$ by $[k] = \frac{q^k - q^{-k}}{q - q^{-1}}$. Likewise, we also have the *quantum factorial* $[k]! = \prod_{i=1}^{k}[i]$ with the convention that $[0]! = 1$. The Temperley–Lieb algebra is home to distinguished elements called the *Jones–Wenzl projectors*, which serve as building blocks of all quantum invariants. They are characterized by two defining properties.

Definition 5.3. The *n-th Jones–Wenzl projector* $f^{(n)} \in TL_n$ is the unique element such that

1. When $f^{(n)}$ is expressed in terms of the additive basis of crossing-less diagrams, the coefficient of the identity diagram is 1, and

2. $e_i f^{(n)} = f^{(n)} e_i = 0$ for all $i = 1, \ldots, n-1$.

Note that as a consequence, the Jones–Wenzl projectors are idempotents, i.e., $(f^{(n)})^2 = f^{(n)}$. More generally for any $m < n$, if we view $f^{(m)}$ as an element of TL_n by inserting it into any set of consecutive m strands, then $f^{(n)} f^{(m)} = f^{(m)} f^{(n)} = f^{(n)}$. Uniqueness follows as a corollary of this idempotence property, and existence follows from a recursive construction of the projectors. We may define $f^{(1)} = \mathbb{1}$, the identity on one strand, and for $n > 1$, we may define $f^{(n)}$ by the the formula in Figure 21. See [Lic97,

Lemma 13.2] for an inductive proof that the projectors defined in this way satisfy the above two properties.

When q is a complex root of unity, additional properties are satisfied by the Jones–Wenzl projectors that makes them conducive for defining topological invariants. Several of these properties appear throughout Sections 5.2, 5.3, and 6. This basic recipe, adapted to a variety of topological objects and settings, yields *quantum invariants*, including the colored Jones polynomials, the Turaev–Viro invariants, and the Reshetikhin–Turaev invariants. The first of these, the colored Jones polynomials, are not only the subject of the classical volume conjecture, but will also be of importance to us in the following sections when they are extended to the setting of knotted trivalent graphs. For now, we define the colored Jones polynomials for framed links.

Definition 5.4. A *framed link* L in a manifold M is a smooth embedding of annuli $\bigsqcup_{i=1}^{k}(S^1 \times [0,1])_{(i)} \hookrightarrow M$ such that L is identified with the $S^1 \times \{0\}$. We refer to the $S^1 \times \{1\}$, as the *framing curves* of L.

Definition 5.5. Let L be a framed link with k components, and let $\mathbf{a} = (a_1, \ldots, a_k)$ be a k-tuple of nonnegative integers. For $i = 1, \ldots, k$, cable the i-th component of L by a_i; that is, replace the component with a_i parallel copies embedded on the framing annulus. Next, take a diagram for the cabled link and insert a copy of $f^{(a_i)}$ into the a_i strands. The result is an element of $\mathcal{S}(S^2)$, which we denote by $L(a_1, \ldots, a_k)$. The $\mathbf{a}$-*colored Kauffman bracket* of L, written either $\langle L \rangle_{\mathbf{a}}$ or $\langle f^{(a_1)}, \ldots, f^{(a_k)} \rangle_L$, is defined by

$$\langle L \rangle_{\mathbf{a}} = \langle L(a_1, \ldots, a_k) \rangle, \tag{41}$$

where the Kauffman bracket is extended to $\mathcal{S}(S^2)$ linearly. When it is understood that all nonnegative integer colors are equal, say, to the number n, we will simply write

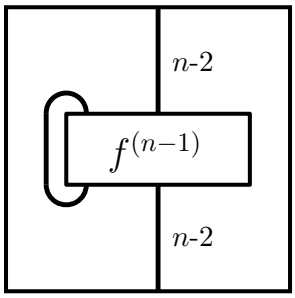

Figure 22: The partial trace of a Jones–Wenzl projector.

$\langle L \rangle_n$ for short. For n a nonnegative integer, we obtain the *n-colored Jones polynomial*, we take the n-colored Kauffman bracket and normalize by setting

$$J_n(L) = (-q)^{-(\frac{n^2+2n}{2})w(D)} \langle D \rangle_n \Big|_{q=t^{-\frac{1}{2}}}. \tag{42}$$

Remark 5.6. The fact that the colored Jones polynomials are truly polynomials follows from the construction and properties of the Jones–Wenzl projectors. In particular, when inserted into a link diagram, the idempotence property turns the right-hand picture in Figure 21 into a *partial trace*, seen in Figure 22. Observe that this partial trace satisfies the second property of Definition 5.3. Namely, it is killed by the turn-backs $e_1, \ldots, e_{n-3}$ in TL_{n-2}. Thus, by uniqueness, we have that the partial trace is a scalar multiple of $f^{(n-2)}$. As in the proof of [Lic62, Lemma 13.2], we may show inductively that the multiplicative factor is $\frac{[n]}{[n-1]}$ for $n > 1$. This cancels the factor $\frac{[n-1]}{[n]}$, yielding a modified expression for $f^{(n)}$ which is clearly polynomial. The same does not necessarily hold when the colored Jones invariant is extended to KTGs.

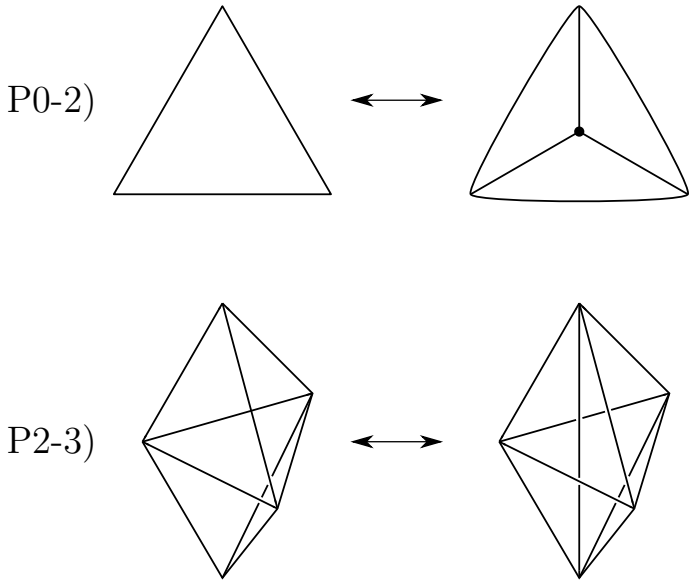

Figure 23: Top: The 0-2 Pachner move. Bottom: The 2-3 Pachner move. Aside from the inner vertex introduced by the 0-2 move, the vertices may or may not be truncated.

5.2 The Relative Turaev–Viro invariants

Quantum invariants do not exist solely for links and graphs. The Turaev–Viro invariants, introduced in [TV92], are quantum invariants defined for compact, oriented 3-manifolds in terms of their triangulations.

Definition 5.7. Let M be a compact, oriented 3-manifold whose boundary may be empty or nonempty. A *partially ideal triangulation* $\mathcal{T}$ of M is a collection of Euclidean tetrahedra, some of whose vertices are truncated, together with face pairings given by affine homeomorphisms. Furthermore, if M has nonempty boundary, then ∂M must be comprised of only the truncation faces.

Vertices and edges of $\mathcal{T}$ which are not contained in truncation faces are called *inner*. We denote the sets of inner vertices and inner edges by V and E, respectively, and the set of tetrahedra by T.

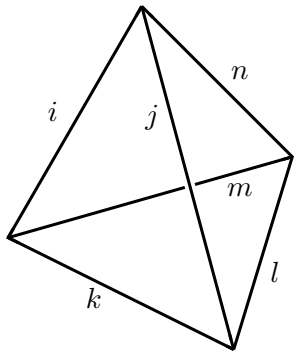

Figure 24: A tetrahedron with edges corresponding to an admissible 6-tuple.

Two triangulations may differ in terms of their combinatorial data, but we consider them to be equivalent if the respective gluings yield the same 3-manifold up to homeomorphism. Much like the Reidemeister moves for links, two triangulations are equivalent if and only if they are related by a finite sequence of the two Pachner moves of Figure 23, as shown in [Pie88]. Several ingredients will be required to obtain invariance under these moves, which we define first.

Definition 5.8. Let $r \geq 3$ be an integer. A *coloring* of a partially ideal triangulation $\mathcal{T}$ is an assignment $\mathbf{a} : E \to \{0, 1, 2, \ldots, r-2\}$.

A triple of colors (i, j, k) is *r-admissible* if

1. $i + j \geq k$, $j + k \geq i$, and $k + i \geq j$,

2. $i + j + k$ is even, and

3. $i + j + k \leq 2(r-2)$.

A 6-tuple of colors (i, j, k, l, m, n) is *r-admissible* if each of the triples (i, j, k), (i, m, n), (j, l, n), and (k, l, m) are r-admissible. Note that these triples correspond to the faces of a tetrahedron, as seen in Figure 24.

Finally, we say that a coloring of a partially ideal triangulation $\mathcal{T}$ is *r-admissible* if every tetrahedron is colored with an admissible 6-tuple.

Remark 5.9. Definition 5.8 corresponds to the $SU(2)$-version of the Turaev–Viro invariants. For $r \geq 3$ an odd integer, an $SO(3)$ coloring is an assignment to even labels only, i.e., a map $\mathbf{a} : E \to \{0, 2, 4, \ldots, r-3\}$. The definition of $SO(3)$ r-admissibility mirrors that of of the $SU(2)$-version.

The building blocks of the Turaev–Viro invariants are defined as follows. For an admissible triple (i, j, k), we define

$$\Delta(i,j,k) = \sqrt{\frac{[s-i]![s-j]![s-k]!}{[s+1]!}}, \tag{43}$$

where $s = \frac{i+j+k}{2}$. For an admissible 6-tuple (i, j, k, l, m, n), we define the *quantum 6j-symbol*

$$\begin{vmatrix} i & j & k \\ l & m & n \end{vmatrix} = \sqrt{-1}^{-\lambda} \prod_{k=1}^{4} \Delta(f_k) \sum_{z=\max\{T_1,T_2,T_3,T_4\}}^{\min\{Q_1,Q_2,Q_3\}} \frac{(-1)^z [z+1]!}{\prod_{i=1}^{4}[z-T_i]! \prod_{i=1}^{3}[Q_i - z]!}, \tag{44}$$

where

- $\lambda = i + j + k + l + m + n$
- $f_1 = (i, j, k)$, $f_2 = (i, m, n)$, $f_3 = (j, l, n)$, and $f_4 = (k, l, m)$,
- $T_1 = \frac{i+j+k}{2}$, $T_2 = \frac{i+m+n}{2}$, $T_3 = \frac{j+l+n}{2}$, and $T_4 = \frac{k+l+m}{2}$, and
- $Q_1 = \frac{i+j+l+m}{2}$, $Q_2 = \frac{i+k+l+n}{2}$, and $Q_3 = \frac{j+k+m+n}{2}$.

Note that the f_i and T_i terms correspond to the four triangular faces of a tetrahedron, as in Figure 24. Likewise, the Q_i terms correspond to the three quadrilaterals which

separate pairs of opposite vertices. As we will see later in the proof of Proposition 5.17, $\Delta(i,j,k)$ and the $6j$-symbol are strongly related to the quantum evaluations of the theta and tetrahedron graphs. We take a moment to recall these, whose values first appeared in [MV94].

Definition 5.10. For an r-admissible triple (i,j,k), there is a unique way of cabling the edges of the theta graph by the i-th, j-th, and k-th Jones–Wenzl projectors and matching up the resulting strands at each vertex. Denote the resulting sum of links by  . We define

$$\theta(i,j,k) := \left\langle \right\rangle = (-1)^s \frac{[s+1]![s-i]![s-j]![s-k]!}{[i]![j]![k]!}, \tag{45}$$

where the Kauffman bracket is extended linearly.

Likewise, for an r-admissible 6-tuple (i,j,k,l,m,n), there is a unique way of cabling the edges of the tetrahedron graph by the corresponding projectors, which we denote by 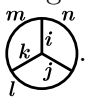 . The value of the cabled tetrahedron is

$$\left\langle \right\rangle = \frac{\prod_{a,b}[Q_b - T_a]!}{[i]![j]![k]![l]![m]![n]!} \sum_{z=\max\{T_1,T_2,T_3,T_4\}}^{\min\{Q_1,Q_2,Q_3\}} \frac{(-1)^z[z+1]!}{\prod_{i=1}^4[z-T_i]!\prod_{i=1}^3[Q_i-z]!}. \tag{46}$$

Finally, we are ready to state the definition of the Turaev–Viro invariants. The proof of invariance under the Pachner moves appears in [CY18, Theorem 2.6] and results from certain symmetries of the $6j$-symbols. We omit this proof since we will be primarily concerned with the relative version of these invariants (see Definition 5.13), which are not strictly 3-manifold invariants as they will depend on the choice of triangulation $\mathcal{T}$.

Definition 5.11. Let M be a compact, oriented 3-manifold, and fix any partially ideal triangulation $\mathcal{T}$ of M. Let $r \geq 3$ an integer, and q be a $2r$-th root of unity such that q^2 is primitive. The $SU(2)$-version *r-th Turaev–Viro invariant* of M is defined by

$$TV_r(M) = \eta_r^{2|V|} \sum_{\mathbf{a} \in A_r} \prod_{i=1}^{|E|} (-1)^{a_i} [a_i + 1] \prod_{s=1}^{|T|} \begin{vmatrix} a_{s_i} & a_{s_j} & a_{s_k} \\ a_{s_l} & a_{s_m} & a_{s_n} \end{vmatrix}, \tag{47}$$

where $\eta_r = \frac{2\sin(\frac{\pi}{r})}{\sqrt{2r}}$. The sum is taken over the set A_r of all r-admissible colorings of $\mathcal{T}$, and $\{a_{s_i}, \ldots, a_{s_n}\}$ are the colors assigned by $\mathbf{a}$ to the edges of the tetrahedron t_s corresponding to Figure 24.

For odd $r \geq 3$, the $SO(3)$-version is defined by

$$TV'_r(M) = (\eta'_r)^{2|V|} \sum_{\mathbf{a} \in A'_r} \prod_{i=1}^{|E|} (-1)^{a_i} [a_i + 1] \prod_{s=1}^{|T|} \begin{vmatrix} a_{s_i} & a_{s_j} & a_{s_k} \\ a_{s_l} & a_{s_m} & a_{s_n} \end{vmatrix}, \tag{48}$$

where $\eta'_r = \frac{2\sin(\frac{2\pi}{r})}{\sqrt{r}}$ and A'_r is the set of all $SO(3)$ r-admissible colorings of $\mathcal{T}$.

In [CY18], Chen and Yang computed the Turaev–Viro invariants for several manifolds with simple triangulations. After observing behavior reminiscent to that of the volume conjecture, they formulated Conjecture 1.2, which we recall.

Conjecture 1.2. *[CY18, Conjecture 1.1] Let M be a hyperbolic 3-manifold. Then for r running over odd integers and $TV_r(M)$ evaluated at $q = e^{\frac{2\pi i}{r}}$,*

$$\lim_{r \to \infty} \frac{2\pi}{r} \ln(TV_r(M)) = \mathit{Vol}(M). \tag{2}$$

The first cases of this conjecture were proven in [DKY18] for M being the figure-eight knot complement or the Borromean rings complement. The authors also proved the

following result relating the $SU(2)$- and $SO(3)$-versions, which also holds for the relative version of the invariants.

Proposition 5.12. *For $r \geq 3$ odd, $TV_r(M) = 2^{b_2(M)} TV'_r(M)$, where $b_2(M)$ is the second $\mathbb{Z}_2$-Betti number of M.*

As the two versions differ by only a constant, we may use either version when studying Conjecture 1.2. We will find, however, that it is often more convenient to work with even colors only, so we will work with the $SO(3)$-version throughout Section 6.

As a potential route to proving Conjecture 1.2, Yang [Yan21] defined a relative version of the Turaev–Viro invariants and proposed an analogous conjecture. Yang defined the relative invariants for ideal triangulations without inner vertices, but we revise the definition to allow for inner vertices.

Definition 5.13. Let M be a compact, oriented 3-manifold, and fix any partially ideal triangulation $\mathcal{T}$ of M. Let $r \geq 3$ an integer, and q be a $2r$-th root of unity such that q^2 is primitive. The $SU(2)$-version of the *r-th relative Turaev–Viro invariant* of $(M, \mathcal{T})$ with the coloring $\mathbf{b} = (b_1, \ldots, b_{|E|})$ on the edges is defined by

$$TV_r(M, \mathcal{T}, \mathbf{b}) = \eta_r^{2|V|} \sum_{\mathbf{a} \in A_r} \prod_{i=1}^{|E|} H(a_i, b_i) \prod_{s=1}^{|T|} \begin{vmatrix} a_{s_i} & a_{s_j} & a_{s_k} \\ a_{s_l} & a_{s_m} & a_{s_n} \end{vmatrix}, \tag{49}$$

where,

$$H(a_i, b_i) = (-1)^{a_i + b_i} \frac{q^{(a_i+1)(b_i+1)} - q^{-(a_i+1)(b_i+1)}}{q - q^{-1}}. \tag{50}$$

For odd $r \geq 3$, the $SO(3)$-version is defined by

$$TV'_r(M, \mathcal{T}, \mathbf{b}) = (\eta'_r)^{2|V|} \sum_{\mathbf{a} \in A'_r} \prod_{i=1}^{|E|} H(a_i, b_i) \prod_{s=1}^{|T|} \begin{vmatrix} a_{s_i} & a_{s_j} & a_{s_k} \\ a_{s_l} & a_{s_m} & a_{s_n} \end{vmatrix}, \tag{51}$$

Conjecture 5.14. *[Yan21, Conjecture 1.3] Let $\{\boldsymbol{b}^{(r)}\}$ be a sequence of colorings of $(M, \mathcal{T})$. For each $i \in \{1, \ldots, |E|\}$, let*

$$\theta_i = \left| 2\pi - \lim_{r\to\infty} \frac{4\pi b_i^{(r)}}{r} \right|, \tag{52}$$

and let $\theta = (\theta_1, \ldots, \theta_{|E|})$.

Let M be a compact, oriented 3-manifold. Then for r running over odd integers and $TV_r(M, \mathcal{T}, \boldsymbol{b}^{(r)})$ evaluated at $q = e^{\frac{2\pi i}{r}}$,

$$\lim_{r\to\infty} \frac{2\pi}{r} \ln\left(TV_r(M, \mathcal{T}, \boldsymbol{b}^{(r)})\right) = Vol(M_{E_\theta}), \tag{53}$$

where M_{E_θ} is M with the hyperbolic polyhedral metric on $(M, \mathcal{T})$ with cone angles θ.

Note that choosing the colors to all be zero recovers Conjecture 1.2 since $TV_r(M) = TV_r(M, \mathcal{T}, (0, \ldots, 0))$ and all cone angles are 2π, making $M_{E_\theta} = M$. In [Yan21], Yang verifies Conjecture 5.14 for all $(M, \mathcal{T}, \mathbf{b}^{(r)})$ yielding manifolds M_{E_θ} having sufficiently small cone angles and nonempty boundary. This opens a potential route to proving Conjecture 1.2 for hyperbolic manifolds with totally geodesic boundary, provided that one is able to show that the cone angles can be deformed from sufficiently small to 2π. However, we will show that the relative Turaev–Viro invariants have a separate use. There are many non-compact, 3-manifolds which can be given relatively simple hyperbolic structures, albeit with only partially geodesic boundaries. These manifolds are non-compact, and as such are out of the scope of the classical Turaev–Viro invariants as well as Conjecture 1.2. Despite this, we are able to realize them as one of the resulting manifolds M_{E_θ} and study them via the relative invariants. What we speak of are the "outsides" of KTGs, first introduced in [Vee09]. To avoid distracting

the reader from the topic of quantum invariants, we will postpone the discussion of KTG outsides to Section 5.5.

5.3 The Reshetikhin–Turaev invariants

To study KTG outsides via the relative Turaev–Viro invariants, we will adapt the approach taken in [DKY18], which is twofold. First, we relate the Turaev–Viro invariants to the Reshetikhin–Turaev invariants through a theorem of Roberts. Second, we express the Reshetikhin–Turaev invariants in terms of the colored Jones evaluation of the KTG. Following [Vee09], we will strategically choose the sequence of colors $\mathbf{b}^{(r)}$ in Theorem 5.14 to yield a simpler computation, but this will also have the effect of making M_{E_θ} homeomorphic to the outside of a KTG. Before this, let us state the definition of the Reshetikhin–Turaev invariants as well as Roberts's Theorem, both appearing in [Yan21].

The Reshetikhin–Turaev invariants are a family of 3-manifold invariants that are defined in terms of surgery. A 1-surgery on a 3-manifold M is the process of removing embedded copies of $S^1 \times D^2$ from M and gluing in copies of $D^2 \times S^1$ via homeomorphisms on the shared toroidal boundary components to obtain a new manifold M'. A convenient way to encapsulate the data necessary to describe a surgery is through a framed link.

The link, itself, determines the core circles of each $S^1 \times D^2$ being removed, while the framing determines the boundary homeomorphisms by demanding that the framing curves bound disks in each $D^2 \times S^1$ being attached. By the Lickorish–Wallace Theorem [Wal60], [Lic62], given any closed oriented 3-manifold M, there exists a framed link $L' \subset S^3$ which yields M via surgery. Two framed links yield the same manifold this

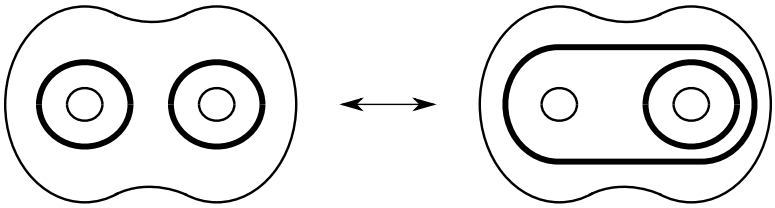

Figure 25: The handle slide, which takes place in any 2-holed annular neighborhood of two link components.

way if and only if they differ by a finite sequence of two moves: the addition or removal of ± 1-framed unknots and the *handle slide*, seen in Figure 25.

Definition 5.15. Fix an integer $r \geq 3$ and a $4r$-th root of unity q. Let M be a closed oriented 3-manifold containing an embedded framed link L, and let $\mathbf{a} : \{L_1, \ldots, L_k\} \to \{0, 1, \ldots, r-2\}$ be a coloring of L, where k is the number of components of L. Let $L' \subset S^3$ be the framed link yielding M via surgery, and let $L'' \subset S^3$ be the preimage of $L \subset M$ before this surgery. The $SU(2)$-version of the r-th relative Reshetikhin–Turaev invariant is

$$RT_r(M, L, \mathbf{a}) = \eta_r \langle \Omega_r, \ldots, \Omega_r, f^{(a_1)}, \ldots, f^{(a_{|L|})} \rangle_{L' \cup L''} \langle \Omega_r \rangle_{U_+}^{-\sigma(L')}, \tag{54}$$

where $\Omega_r = \eta_r \sum_{i=0}^{r-2} (-1)^i [i+1] f^{(i)}$, U_+ is the $+1$-framed unknot, and $\sigma(L')$ is the signature of the linking matrix of L'.

For odd $r \geq 3$, the $SO(3)$-version is defined for $\mathbf{a} : \{L_1, \ldots, L_{|L|}\} \to \{0, 2, \ldots, r-3\}$ by

$$RT'_r(M, L, \mathbf{a}) = \eta'_r \langle \Omega'_r, \ldots, \Omega'_r, f^{(a_1)}, \ldots, f^{(a_{|L|})} \rangle_{L' \cup L''} \langle \Omega'_r \rangle_{U_+}^{-\sigma(L')}, \tag{55}$$

where $\Omega'_r = \eta'_r \sum_{i=0,\ i \text{ even}}^{r-3} [i+1] f^{(i)}$.

Invariance follows from the fact that $\langle a \rangle_{U_-} = \langle a \rangle_{U_+}^{-1}$ for all colors a, taken into account by the normalization factor, and the fact that the elements Ω_r and Ω_r' are specially designed to allow for handle slides, which do not affect the link signature (see [Lic97, Chapter 13]).

Remark 5.16. Immediately from the definition, some key properties of the classical Reshetikhin–Turaev invariants carry over to the relative version as well. In particular, we have that $RT_r(S^2 \times S^1, \emptyset) = 1$ and $RT_r(S^3, \emptyset) = \eta_r$, and more generally that $RT_r(S^3, L, \mathbf{a}) = \eta_r \langle a_1, \ldots, a_{|L|} \rangle_L$. For a connected sum, we have

$$RT_r(M_1 \# M_2, L_1 \cup L_2, (\mathbf{a}_1, \mathbf{a}_2)) = \eta_r^{-1} RT_r(M_1, L_1, \mathbf{a}_1) RT_r(M_2, L_2, \mathbf{a}_2), \tag{56}$$

where the links L_1 and L_2 are disjoint from the 2-spheres used to construct the connected sum. Analogous properties hold for the $SO(3)$-version.

The classical Turaev–Viro invariants are related to the Reshetikhin–Turaev invariants by a theorem of Roberts [Rob95, Theorem 3.7], itself an extension of an earlier result by Turaev and Walker. In [Yan21], Yang sketches the proof of a generalization of Roberts's theorem to the relative setting. We state this version of the theorem as well as the full proof.

Theorem 5.17. *[Yan21, Theorem 1.2] At* $q = e^{\frac{\pi i}{r}}$*,*

$$TV_r(M, \mathcal{T}, \boldsymbol{b}) = (\eta_r)^{(v_{inn} - \chi(M))} RT_r(D(M'), D(E), \boldsymbol{b}), \tag{57}$$

and at $q = e^{\frac{2\pi i}{r}}$ *for odd* r*,*

$$TV_r'(M, \mathcal{T}, \boldsymbol{b}) = (\eta_r')^{(v_{inn} - \chi(M))} RT_r'(D(M'), D(E), \boldsymbol{b}), \tag{58}$$

where M' is the 3-manifold obtained by puncturing M at every inner vertex of $\mathcal{T}$, $D(M') = M' \cup_{\partial M'} (-M')$ denotes the double of M', and $D(E)$ denotes the framed link obtained by doubling the edges of $\mathcal{T}$, which inherits the coloring $\boldsymbol{b}$.

Proof. We will prove only the $SO(3)$-case, since that is what the results of Section 6 will deal with, but the $SU(2)$-case is similar. First, we will identify a link $L(M, \mathcal{T}, \mathbf{b})$, called a *chain-mail link*, whose quantum evaluation realizes the r-th relative Turaev–Viro invariant.

Consider the handle decomposition of M dual to $\mathcal{T}$, whose 0-handles are balls contained in the interior of each tetrahedron, and whose 1-, 2-, and 3-handles are regular neighborhoods of the faces, edges, and inner vertices, respectively. Let H be the handlebody consisting of the union of the 0- and 1-handles. Let $\{\delta_1, \ldots, \delta_{|F|}\}$ be meridians of the 1-handles and $\{\epsilon_1, \ldots, \epsilon_{|E|}\}$ be the attaching circles for the 2-handles, pushed slightly into H, and give these curves the blackboard framing with respect to H. Let $\{\gamma_1, \ldots, \gamma_{|E|}\}$ be small 0-framed trivial loops linking the respective $\{\epsilon_i\}$. Cable the $\{\delta_i\}$ and $\{\epsilon_i\}$ by Ω'_r, and cable γ_i by the b_i-th Jones–Wenzl projector. Let $L(M, \mathcal{T}, \mathbf{b})$ be the union of the framed, cabled δ-, ϵ-, and γ- curves. Refer to Figure 26 for an illustration of $L(M, \mathcal{T}, \mathbf{b})$.

Note that since the 3-handles are not used in the construction of the chain-mail link, we have $L(M, \mathcal{T}, \mathbf{b}) = L(M', \mathcal{T}, \mathbf{b})$. We set

$$CM'_r(M, \mathcal{T}, \mathbf{b}) = (\eta'_r)^{d_0+d_3} \langle L(M, \mathcal{T}, \mathbf{b}) \rangle \big|_{q=e^{\frac{2\pi i}{r}}}, \tag{59}$$

where d_0 and d_3 are the numbers of 0- and 3-handles in the dual handle decomposition, respectively. In [Rob95], it is shown that the non-relativized version of (59) does not depend on the handle decomposition used in its construction. This will not be the case

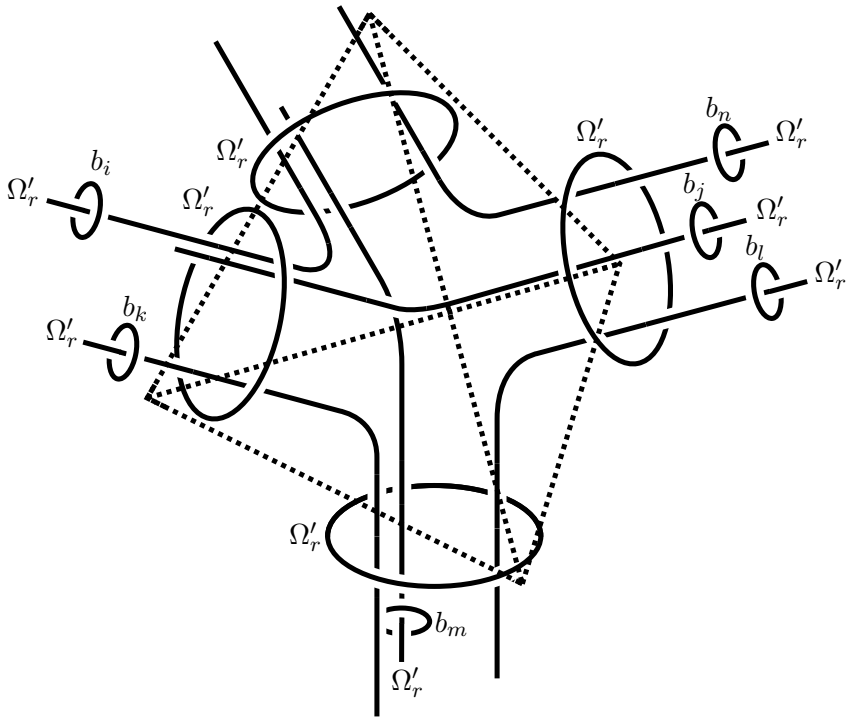

Figure 26: The chain-mail link corresponding to the handle decomposition dual to a partially ideal triangulation.

for the relativized chain-mail link, which is defined only for handle decompositions dual to partially ideal colored triangulations, but this will not pose an issue provided we stick to using only that handle decomposition.

Referring to Definition 5.10, when the edges of a triangular face f are colored (i, j, k), we will write $\theta(f)$ as shorthand for $\theta(i, j, k)$, and when the edges of a tetrahedron t are colored (i, j, k, l, m, n), we will write $\langle t \rangle$ as shorthand for $\left\langle \right.$ 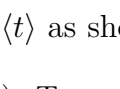 $\left. \right\rangle$. We claim that $CM'_r(M, \mathcal{T}, \mathbf{b}) = (\eta'_r)^{\chi(M)} TV'_r(M, \mathcal{T}, \mathbf{b})$. To see this, consider Figure 26 and the relations in Figure 27. By applying the fusion rule to every δ-curve followed by the

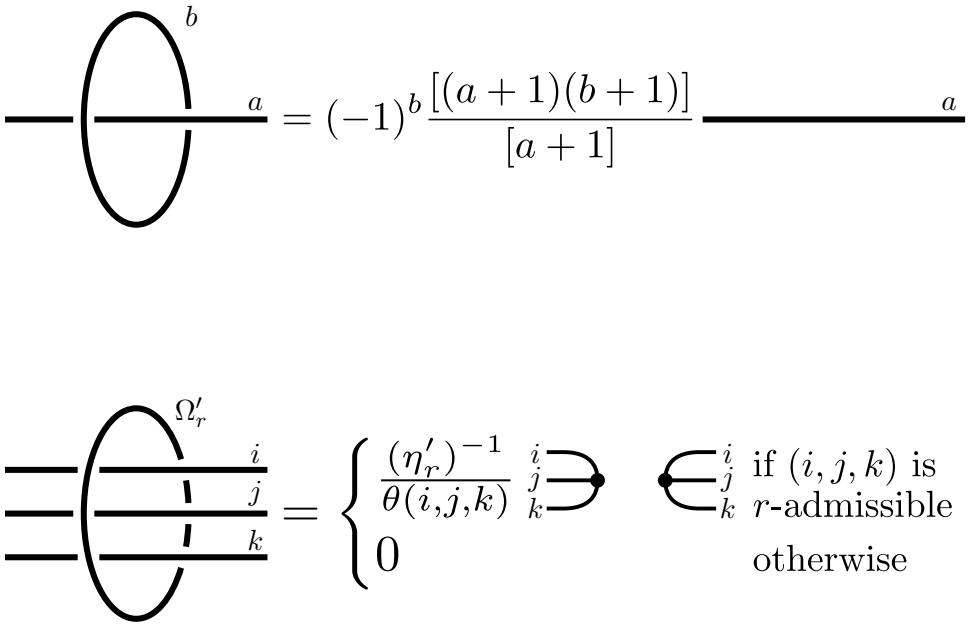

Figure 27: Top: The Hopf link relation. Bottom: The fusion rule.

Hopf link relation to every ϵ_i, γ_i pair, we obtain

$$\begin{aligned} CM'_r(M,\mathcal{T},\mathbf{b}) = (\eta'_r)^{d_0+d_3} \quad & \sum_{\mathbf{a}\in A'_r}\prod_{i=1}^{|E|}(\eta'_r(-1)^{a_i}[a_i+1])\left((-1)^{b_i}\frac{[(a_i+1)(b_i+1)]}{[a_i+1]}\right)\cdot \\ & \prod_{j=1}^{|F|}\frac{(\eta'_r)^{-1}}{\theta(f_j)}\prod_{s=1}^{|T|}\langle t_s\rangle \\ = (\eta'_r)^{d_0-d_1+d_2+d_3} & \sum_{\mathbf{a}\in A'_r}\prod_{i=1}^{|E|}H(a_i,b_i)\prod_{j=1}^{|F|}\theta(f_j)^{-1}\prod_{s=1}^{|T|}\langle t_s\rangle \\ = (\eta'_r)^{\chi(M)+2|V|} \quad & \sum_{\mathbf{a}\in A'_r}\prod_{i=1}^{|E|}H(a_i,b_i)\prod_{s=1}^{|T|}\left(\prod_{k=1}^{4}\theta(f_{t_s,k})^{-\frac{1}{2}}\right)\langle t_s\rangle\,, \end{aligned}$$

where the last equality is obtained by matching each face to the two tetrahedra in which it appears ($f_{t_s,k}$ denotes the k-th face of the tetrahedron t_s). Observe that once we know a face lies in a certain tetrahedron t_s, we can rewrite the value of the theta symbol in (45) as

$$\theta(f_{t_s,1}) = \theta(i,j,k) = (\sqrt{-1})^{T_1} \frac{[T_1-i]![T_1-j]![T_1-k]![T_1+1]!}{[i]![j]![k]!}$$
$$= (\sqrt{-1})^{T_1} \frac{[Q_3-T_2]![Q_2-T_3]![Q_1-T_4]![T_1+1]!}{[i]![j]![k]!},$$

where the quantities T_a and Q_b were defined below (44) with reference to Figure 24. We may obtain similar expressions for the remaining three theta symbols $\theta(f_{t_s,k}),\ k = 2,3,4$. Therefore,

$$CM'_r(M,\mathcal{T},\mathbf{b}) = (\eta'_r)^{\chi(M)+2|V|} \sum_{\mathbf{a}\in A'_r} \prod_{i=1}^{|E|} H(a_i,b_i) \cdot$$
$$\prod_{t\in T} (\sqrt{-1})^{-\lambda} \frac{[a_{t_i}]![a_{t_j}]![a_{t_k}]![a_{t_l}]![a_{t_m}]![a_{t_n}]!}{\sqrt{\prod_{a,b}[Q_b-T_a]! \prod_{k=1}^{4}[T_k+1]!}} \langle t \rangle$$
$$= (\eta'_r)^{\chi(M)+2|V|} \sum_{\mathbf{a}\in A'_r} \prod_{i=1}^{|E|} H(a_i,b_i) \prod_{s=1}^{|T|} \begin{vmatrix} a_{s_i} & a_{s_j} & a_{s_k} \\ a_{s_l} & a_{s_m} & a_{s_n} \end{vmatrix}$$
$$= (\eta'_r)^{\chi(M)} \qquad TV'_r(M,\mathcal{T},\mathbf{b}),$$

where the second-to-last equality is obtained by evaluating the tetrahedron graph as in 46.

On the other hand, by investigating the 3-manifold obtained by surgery on $L(M,\mathcal{T},\mathbf{b})$, we will also be able to conclude that $CM'_r(M,\mathcal{T},\mathbf{b}) = (\eta'_r)^{v_{\text{inn}}} RT'_r(D(M'),D(E),\mathbf{b})$. Following [Rob95, Theorem 3.7], we begin by constructing two relevant 4-manifolds with homeomorphic boundaries, W_1 and W_2. Let V_1 be obtained by attaching $|F|$ 4-dimensional 1-handles to B^4 along the δ-curves in $S^3 = \partial B^4$, and let V_2 be obtained by attaching 2-handles instead. Note that we can alternatively view V_1 as the result

of removing $|F|$ copies of $D^2 \times D^2$ from the inside of B^4, while V_2 is the result of gluing $|F|$ copies of $D^2 \times D^2$ to the outside of B^4. Thus, $\partial V_1 \cong \partial V_2 \cong \#_{i=1}^{|F|} S^2 \times S^1$. We complete the constructions by letting W_1 and W_2 be obtained by attaching 4-dimensional 2-handles along the ϵ-curves in V_1 and V_2, respectively, and disjointly from the previously attached handles. Thus, we have $\partial W_1 \cong \partial W_2$ as well.

Now, we can identify W_1 by comparing its handle decomposition to the one for M which is dual to $\mathcal{T}$. Write

$$M = H_1^0 \cup \cdots \cup H_{|T|}^0 \cup H_1^1 \cup \cdots \cup H_{|F|}^1 \cup H_1^2 \cup \cdots \cup H_{|E|}^2 \cup H_1^3 \cup \cdots \cup H_{v_{\text{inn}}}^3, \quad (60)$$

and

$$W_1 = G_1^0 \cup G_1^1 \cup \cdots \cup G_{|F|}^1 \cup G_1^2 \cup \cdots \cup G_{|E|}^2, \quad (61)$$

where H_k^d is a 3-dimensional d-handle and G_k^d is the corresponding 4-dimensional d-handle. Since $G_k^d \cong H_k^d \times I$ with consistent gluings, we can see that $W_1 \cong (M' \times I) \natural (B^3 \times S^1)^{\natural(|F|-g(H))}$. The reason for the $|F| - g(H)$ copies of $B^3 \times S^1$ is the presence of the redundant 1-handles for W_1, only $g(H) = 1 + |T|$ of which are required to produce $H \times I$, where H is the handlebody previously defined for M. Therefore, $\partial W_1 \cong \partial W_2 \cong D(M') \# (S^2 \times S^1)^{\#(|F|-g(H))} = D(M') \# (S^2 \times S^1)^{\#(|T|-1)}$.

Since gluing 4-dimensional 2-handles (as we did in the construction of W_2) corresponds to surgering along a link in the boundary, $D(M') \# (S^2 \times S^1)^{\#(|T|-1)}$ is indeed the 3-manifold obtained by surgering along L', the sublink of $L(M, \mathcal{T}, \mathbf{b})$ consisting of the δ- and ϵ-components. As shown in [Rob95, Theorem 3.7], we have $\sigma(L') = 0$. Note that after surgery, γ_i becomes isotopic to the core of the 2-handle attached along ϵ_i, which is the double of the edge e_i. Hence, we have by Definition 5.15 that

$$\begin{aligned} CM'_r(M,\mathcal{T},\mathbf{b}) &= (\eta'_r)^{|T|+v_{\text{inn}}-1} RT'_r(D(M')\#(S^2\times S^1)^{\#(|T|-1)}, D(E), \mathbf{b}) \\ &= (\eta'_r)^{v_{\text{inn}}} RT'_r(D(M'), D(E), \mathbf{b}), \end{aligned}$$

where the last equality holds by the properties in Remark 5.16 and the fact that the framed link $D(E)$ and the copies of $(S^2 \times S^1)$ are disjoint. □

5.4 The Reshetikhin–Turaev TQFT

A second fact of central importance is the relationship between the relative Reshetikhin–Turaev invariants and the colored Jones polynomial resulting from the TQFT framework of [Bla+95]. This relationship was first explored in [DKY18], where the authors used it to explicitly compute the Turaev–Viro invariants of some link complements, which aided in verifying Conjecture 1.2 for these cases. We take a moment to review the key properties of the TQFT underpinning the relative $SO(3)$ Reshetikhin–Turaev invariants.

Definition 5.18. The $SO(3)$-version of the *Reshetikhin–Turaev topological quantum field theory* (TQFT) is a map V'_r assigning a closed oriented surface Σ containing a colored framed link L to a finite-dimensional $\mathbb{C}$-vector space $V'_r(\Sigma, L, \mathbf{a})$. By a "framed link" in a surface, we mean a collection of oriented closed intervals $L_1, \ldots, L_n$, and a coloring $\mathbf{a} = (a_1, \ldots, a_n)$ of such a link places a_i distinct points on the interval L_i. V'_r satisfies the following axioms:

1. $V'_r(\emptyset) = \mathbb{C}$.

2. $V'_r(-\Sigma, -L, \mathbf{a}) = \overline{V'_r(\Sigma, L, \mathbf{a})}$.

3. $V'_r(\Sigma_1 \sqcup \Sigma_2, L_1 \sqcup L_2, (\mathbf{a}_1, \mathbf{a}_2)) \cong V'_r(\Sigma_1, L_1, \mathbf{a}_1) \otimes V'_r(\Sigma_2, L_2, \mathbf{a}_2)$.

4. V'_r is functorial with respect to cobordisms. In other words, if M is a compact, oriented 3-manifold containing an $\mathbf{a}$-colored framed KTG Γ and $\partial M = \Sigma_1 \sqcup \Sigma_2$, then V'_r induces a linear map

$$Z'_r : V'_r(\Sigma_1, \Gamma \cap \Sigma_1, \mathbf{a}'_1) \to V'_r(\Sigma_2, \Gamma \cap \Sigma_2, \mathbf{a}'_2),$$

   where $\mathbf{a}'_1$ and $\mathbf{a}'_2$ are induced by $\mathbf{a}$. In particular, if $\partial M = \Sigma$, then we have a unique vector $Z'_r(M, \Gamma, \mathbf{a}) \coloneqq Z'_r(1) \in V'_r(\Sigma, \Gamma \cap \Sigma, \mathbf{a}')$.

5. There is a non-degenerate hermitian sesquilinear pairing $\langle \cdot, \cdot \rangle'_r$ such that if $\partial(M_1, \Gamma_1) = \partial(M_2, \Gamma_2) = (\Sigma, \Gamma_1 \cap \Sigma)$, then

$$RT'_r(M_1 \cup_\Sigma (-M_2), \Gamma_1 \cup (-\Gamma_2), \mathbf{a}') = \langle Z'_r(M_1, \Gamma_1, \mathbf{a}_1), Z'_r(M_1, \Gamma_1, \mathbf{a}_2) \rangle'_r,$$

   provided the colors agree $\Gamma_1 \cap \Sigma$.

The $SU(2)$-version is defined analogously.

When considering KTGs, the most important of these vector spaces to us will be the TQFT of the 2-sphere containing a 2- or 3-component framed link respectively colored by (i, j) or (i, j, k), which we will denote as either $V'_r(S^2(i, j))$ or $V'_r(S^2(i, j, k))$, and also the TQFT of the solid torus, $V'_r(D^2 \times S^1)$. Fortunately, these vector spaces are well-understood.

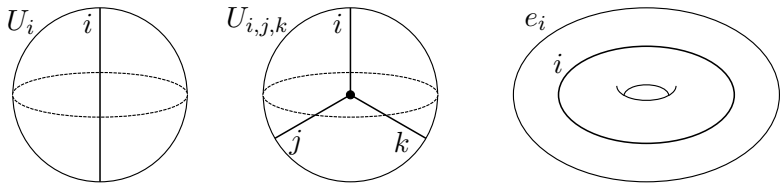

Figure 28: The colored graphs which generate the TQFTs of Proposition 5.19.

Proposition 5.19. *[Bla+95, Theorem 1.15, Corollary 4.10] We have*

$$rank(V_r'(S^2(i,j))) = \begin{cases} 1 & \text{if } i = j \\ 0 & \text{if } i \neq j \end{cases},$$

$$rank(V_r'(S^2(i,j,k))) = \begin{cases} 1 & \text{if } (i,j,k) \text{ is } r\text{-admissible} \\ 0 & \text{otherwise} \end{cases}, \text{ and}$$

$$rank(V_r'(D^2 \times S^1)) = \frac{r-1}{2}.$$

Furthermore, when $i = j$, $V_r'(S^2(i,j))$ is generated by $U_i \coloneqq Z_r'(B^3, I, (i))$, where I denotes the axis of B^3. Likewise, when (i,j,k) is admissible, $V_r'(S^2(i,j,k))$ is generated by $U_{i,j,k} \coloneqq Z_r'(B^3, Y, (i,j,k))$, where Y denotes the tripod graph. Lastly, $V_r'(D^2 \times S^1)$ is generated by the basis $\{e_i\}$ given by $e_i \coloneqq Z_r'(D^2 \times S^1, S^1 \times \{0\}, (i))$, where $S^1 \times \{0\}$ denotes the core of $D^2 \times S^1$. Furthermore, this basis is orthonormal with respect to $\langle \cdot, \cdot \rangle_r'$. A visual depiction of these generators can be seen in Figure 28.

5.5 Knotted Trivalent Graphs

In this section, we discuss KTGs and related topics which are relevant to Main Theorem 2.

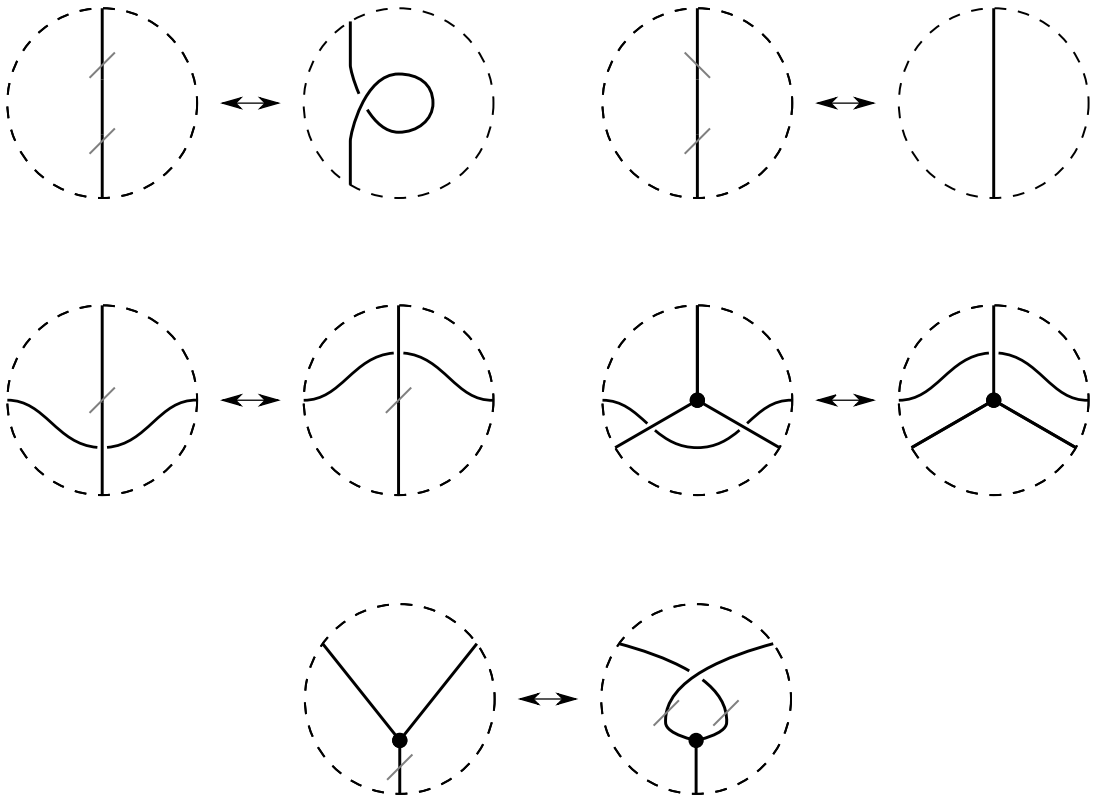

Figure 29: The KTG isotopy moves.

Definition 5.20. A (framed) *knotted trivalent graph* (KTG) is a smooth embedding of a trivalent graph $\Gamma \hookrightarrow S^3$, which is the spine of an embedded ribbon surface. Edges without vertices are allowed, so in particular, all framed links are considered to be KTGs.

Similarly to links, we consider KTGs up to isotopy. The moves of Figure 29 together with the Reidemeister moves determine whether two given diagrams represent isotopic KTGs. When drawing KTG diagrams, we adopt the convention of [Vee09] where instead of drawing the ribbon surface, we use a gray marker to indicate a half-twist along an edge. For instance, the top left diagram in Figure 29 depicts two positive half-twists.

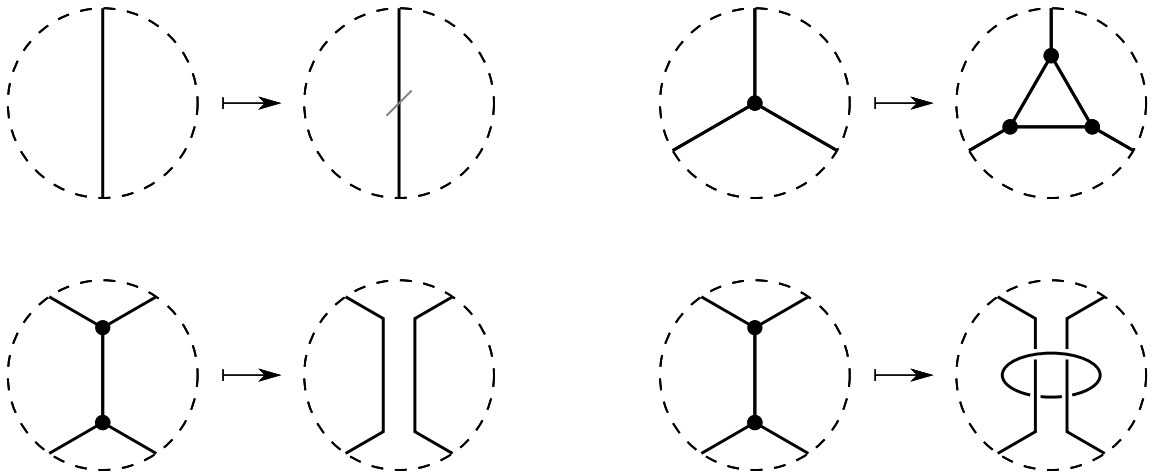

Figure 30: Top left: The positive half-twist, which changes the framing of an edge. Top right: The triangle move. Bottom left: The unzip move. Bottom right: The augmented unzip move.

Van der Veen proved in [Vee09, Theorem 1] than any KTG can be obtained from the standard tetrahedron graph by a sequence of positive/negative half-twist, triangle, and unzip moves, which are depicted in Figure 30. These generating moves are useful in computing quantum evaluations of KTGs as they correspond to the well-known relations of Figure 31, which may be found in [Lic62]. These relations can all be proven skein theoretically. For example, to prove the half-twist relation, one may observe that all but one state of the cabled diagram contain a turn-back, and thus equal zero by Definition 5.3. Observe that the third relation of Figure 31 is the most computationally taxing, which in general turns the quantum evaluation of a KTG into a multi-sum taken over all admissible colorings of a different KTG with some colors predetermined. Augmented KTGs were introduced in [Vee09] in order to simplify this computation under certain conditions. They are obtained as follows:

Definition 5.21. An *augmented KTG* is the result of taking any sequence of KTG generating moves and replacing all of the unzip moves with augmented unzip moves, as seen in the bottom-right of Figure 30. We call the new link components introduced by

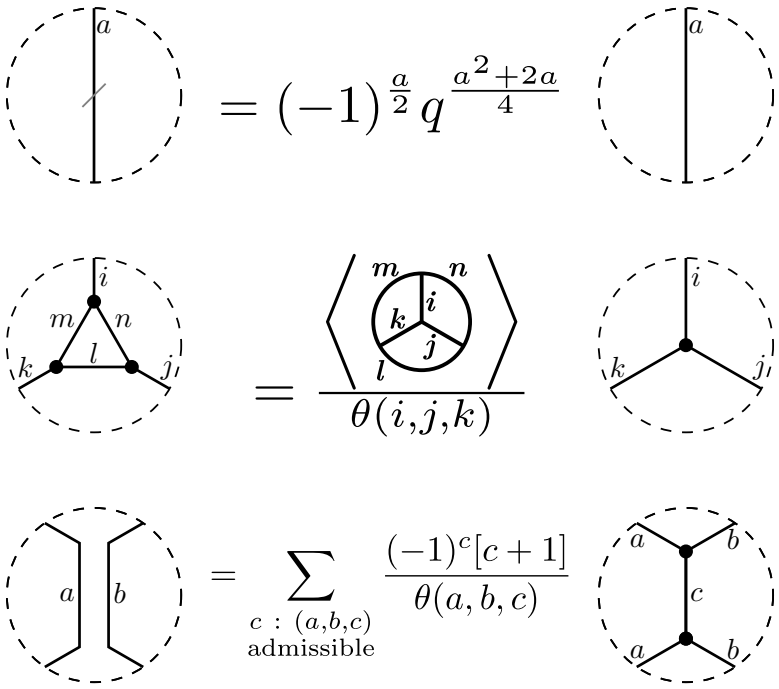

Figure 31: Reversing the KTG generating moves.

the augmented unzip move *augmentation rings*. Write A for the set of augmentation rings.

Observe that the result of unzipping a half-twisted edge is two crossing strands. Note that this is the only way to generate non-nugatory crossings.

In general, the boundary of a KTG complement is a higher-genus surface, and as such the complement cannot be given a complete finite volume hyperbolic structure if the boundary is made to be entirely cusped or entirely geodesic. Instead, we associate to a KTG Γ its *outside* $O(\Gamma)$, defined in [Vee09, Definition 14], which has a partially ideal boundary.

Definition 5.22. The outside of Γ, $O(\Gamma)$, is a 3-manifold obtained by removing an open ball around every vertex of Γ and a closed solid cylinder around every edge (or a closed solid torus for an edge without vertices) from S^3. KTG outsides are

implicitly given a boundary pattern consisting of a simple closed curve around every puncture of the thrice-punctured 2-sphere boundary components of $O(\Gamma)$. If a KTG outside admits a complete hyperbolic structure, then that structure is unique up to homeomorphism provided we restrict ourselves to homeomorphisms which preserve the boundary pattern.

In [Vee09], it is shown that all augmented KTGs have hyperbolic outsides comprised of regular hyperbolic octahedra. The precise value of the volume will be useful to us when proving Corollary 1.5, so we state the full result here.

Proposition 5.23. *[Vee09, Theorem 2, part 2] Let* Γ *be an augmented KTG whose sequence of generating moves contains* t *triangle moves. Then,* $Vol(O(\Gamma)) = (2t+2)v_{oct}$*, where* $v_{oct} \approx 3.66386$ *is the volume of a regular ideal hyperbolic octahedron.*

Van der Veen introduced augmented KTGs and their outsides with the express purpose of stating and proving a version of the volume conjecture for augmented KTGs. The colored Kauffman bracket and colored Jones polynomial may be extended to KTGs as follows: edges of the KTG Γ are assigned an $SU(2)$ or $SO(3)$ coloring $\mathbf{a}$. If $\mathbf{a}$ is admissible, there is a unique way of cabling the edges of Γ by the corresponding Jones–Wenzl projectors, and we define $\langle\Gamma\rangle_{\mathbf{a}}$ by taking the Kauffman bracket of the resulting sum of framed links, extended linearly. Otherwise, if $\mathbf{a}$ is not admissible, we define $\langle\Gamma\rangle_{\mathbf{a}}$ to be zero. We state van der Veen's conjecture here for the completeness of discussion.

Conjecture 5.24. *Let Γ be a KTG and let $J_r(\Gamma) = \frac{\langle \Gamma \rangle_r}{(\langle U \rangle_r)^s}$, where U is the zero-framed unknot and s is the number of split components of Γ. Then, for r running over odd integers and $J_r(\Gamma)$ evaluated at $q = e^{\frac{\pi i}{r}}$,*

$$\lim_{r \to \infty} \frac{2\pi}{r} \ln(|J_n(\Gamma)|) = \mathit{Vol}(O(\Gamma)). \tag{62}$$

In [Vee09, Theorem 2, part 3], it is proven that all augmented KTGs (with a sufficiently large number of additional redundant augmentation rings) satisfy Conjecture 5.24. Note that the KTGs which can be generated solely by triangle moves are a special case of augmented KTGs having zero augmentation rings. For this reason, one may view Corollary 1.5 as a partial extension of this result to the setting of the relative Turaev–Viro invariants. We are finally ready to prove Main Theorem 2.

6 Proof of Main Theorem 2

The goal of this section is to prove Main Theorem 2, which we restate here.

Main Theorem 2. *Let $r \geq 9$ be an odd integer and $\Gamma \subset S^3$ an augmented KTG with v_Γ vertices and $|A|$ augmentation rings. Let M, $\mathcal{T}$, and $\boldsymbol{b}^{(r)}$ be defined as in Section 6.1, and let v_{inn} be the number of inner vertices of $\mathcal{T}$. Then,*

$$TV_r(M, \mathcal{T}, \boldsymbol{b}^{(r)}) = 2^{v_\Gamma + |A| - 1} (\eta_r')^{2-2v_\Gamma} \theta(n,n,n)^{-v_\Gamma} [n+1]^{-v_{inn}} \sum_{\substack{0 \leq \boldsymbol{i} \leq r-3, \\ \boldsymbol{i} \text{ even}}} \left| \langle \Gamma \rangle_{\boldsymbol{i},n} \right|^2, \quad (7)$$

where $\eta_r' = \frac{2\sin(\frac{2\pi}{r})}{\sqrt{r}}$, and $\langle \Gamma \rangle_{\boldsymbol{i},n}$ is the ation of Γ where the augmentation rings are colored by $\boldsymbol{i} = (i_1, \ldots, i_{|A|})$ and all other edges by n.

6.1 Triangulations via augmented KTGs

Recall from Definition 5.13 that the three parameters required by Yang's relative Turaev–Viro invariants are a compact, oriented 3-manifold M, a partially ideal triangulation $\mathcal{T}$ of M, and a sequence of colorings $\mathbf{b}^{(r)}$ of the edges of $\mathcal{T}$. Given an augmented KTG Γ, we will show that Γ can be enhanced into a triangulation by adding extra edges and inner vertices as necessary.

Proposition 6.1. *Let $\Gamma \subset S^3$ be an augmented KTG. Let $\nu(V(\Gamma))$ be an open regular neighborhood of the vertices of Γ and $\nu(A(\Gamma))$ an open regular neighborhood of the augmentation rings. Consider the manifold $M = S^3 \setminus (\nu(V(\Gamma)) \sqcup \nu(A(\Gamma)))$. The edges of Γ form a framed link $L = M \cap E(\Gamma) \subset M$. Let $L' \subset M$ be the (unframed) spine of L. Then, there exists a partially triangulation $\mathcal{T}$ of M such that L' is spanned by $E(\mathcal{T})$.*

Proof. It suffices to first show that we can add extra edges and inner vertices to obtain a *polyhedral* decomposition $\mathcal{P}$ of M with no monogon or bigon faces. Once this has been done, we can break the polyhedra into tetrahedra by the process of "coning to a vertex" as described in [Pur20, Chapter 4.1]. Simply choose any vertex v and add edges between v and all other non-adjacent vertices. Next, create more edges and faces as necessary to ensure that every pair of edges meeting v is contained in a triangular face and every triple of triangles meeting v is contained in a tetrahedron. Split off the resulting tetrahedra and continue exhaustively.

We may assume that Γ lies on the plane $S^2 \subset S^3$ away from augmentation rings and crossings. Our polyhedral decomposition will consist of two identical polyhedra, one lying above S^2 and the other below. We will obtain $\mathcal{P}$ by induction on $|A|$, flattening Γ as we go. For the base case $|A| = 0$, Γ is precisely one of the graphs referenced by Corollary 1.5, ignoring the possible presence of half-twists which do not influence our triangulation. Such graphs are already planar and are free of monogons and bigons, since the triangle move introduces a new triangular face and increases the edge-count of neighboring faces. We define $\mathcal{P}$ by replacing the trivalent vertices of Γ with ideal (i.e., truncated) ones, and we are done.

For the induction step, suppose that Γ is obtained from Γ' by performing a single unzip move on the edge e. Let D be a collection of disjoint embedded disks which are bounded by the augmentation rings of Γ and minimally intersect the rest of Γ. Let $d \in D$ be the disk produced by the new unzip move. Then the interior of d intersects Γ in exactly two points. To flatten Γ, first cut S^3 along d and remove any half-twists that may have been produced by the unzip by performing half-rotations, as in the top image of Figure 32.

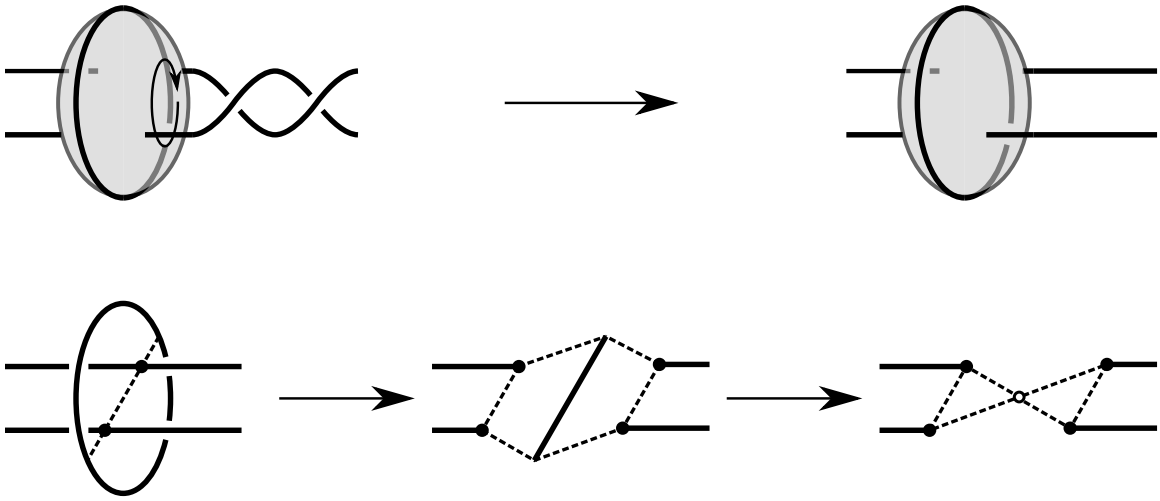

Figure 32: Top: Removal of half-twists. Bottom: Contracting and augmentation ring to an ideal vertex.

Next, re-glue along d and add two inner vertices where $\text{int}(d)$ intersects Γ and three edges where d intersects S^2. To better see the new faces we have created, cut along S^2 and unfold each half-disk, collapsing the arcs of the augmentation ring to ideal vertices. The result is two pairs of triangular faces, one such pair being depicted in the bottom image of Figure 32. The exact face-pairing map on these four faces depends on whether the number of removed half-twists was odd or even.

With these new faces, the polyhedral decomposition of Γ', which exists by assumption, may be extended to one on Γ after one final step. If the edge $e \in E(\Gamma')$ intersected another disk $d' \in D$ at one of our previously created inner vertices before the unzip, then after unzipping, two parallel strands will intersect d' and we replace the original inner vertex with two. In the end, we have created two new triangular faces and some number of rectangular faces between the parallel strands, and the edge-counts of all other faces could only have been increased. Therefore, we have obtained a polyhedral decomposition of M with no monogon or bigon faces. $\square$

Note that the above polyhedral decomposition is similar to the one appearing in [Pur20, Proposition 7.8]. A key difference, however, is that we do not collapse strands of the KTG to ideal vertices, but rather leave them as edges of $\mathcal{T}$, possibly split-up by new inner vertices (this is what is meant by $E(\mathcal{T})$ *spanning* L'). Now that we have defined M and $\mathcal{T}$, the final parameter needed for the relative Turaev–Viro invariants is the sequence of colorings of $\mathcal{T}$. For an odd integer r, let $n = \frac{r\pm 1}{2}$ with the sign chosen so that n is even. Note that when $r \geq 9$, (n, n, n) is an r-admissible triple. Define the coloring $\mathbf{b}^{(r)}$ on $\mathcal{T}$ by assigning the color n to the edges which span L' and 0 to all other edges (i.e., the dotted ones in Figure 32 as well as any created in the coning process). We are now ready to prove Main Theorem 2.

Proof of Main Theorem 2. By Proposition 5.12 and Theorem 5.17, we have that at $q = e^{\frac{2\pi i}{r}}$,

$$\begin{aligned} TV_r(M, \mathcal{T}, \mathbf{b}^{(r)}) &= 2^{b_2(M)}(\eta'_r)^{v_{\text{inn}}-\chi(M)} RT'_r(D(M), D(E), \mathbf{b}^{(r)}) \\ &= 2^{v_\Gamma+|A|-1}(\eta'_r)^{v_{\text{inn}}-v_\Gamma} RT'_r(D(M), D(E), \mathbf{b}^{(r)}). \end{aligned} \tag{63}$$

Applying the color 0, we get

$$RT'_r(D(M), D(E), \mathbf{b}^{(r)}) = RT'_r(D(M), D(L'), (n, \dots, n)). \tag{64}$$

Here, note that we implicitly view $D(L')$ as a banded link in $D(M)$ by taking the blackboard framing with respect to the planar projection, and doubling it along the boundary 2-spheres of M. However, $D(L')$ and $D(L)$ are isotopic in $D(M)$, so we have

$$RT'_r(D(M), D(L'), (n, \dots, n)) = RT'_r(D(M), D(L), (n, \dots, n)),$$

thereby recovering the original framing of L. By the TQFT axioms in Definition 5.18, we have that

$$\begin{aligned} RT'_r(D(M), D(L), (n, \ldots, n)) &= \langle Z'_r(M, L, (n, \ldots, n)), Z'_r(-M, -L, (n, \ldots, n))\rangle'_r \\ &= |Z'_r(M, L, (n, \ldots, n))|^2. \end{aligned} \tag{65}$$

Since Γ was an augmented KTG, we have that $Z'_r(M, L, (n, \ldots, n)) \in V'_r(\partial M, L \cap \partial M, (n, \ldots, n)) = V'_r(S^2(n, n, n))^{\otimes v_\Gamma} \otimes V'_r(S^2(n, n))^{\otimes v_{\text{inn}}} \otimes V'_r(D^2 \times S^1)^{\otimes |A|}$ by Definition 5.18. Proposition 5.19 tells us that $V'_r(\partial M, L \cap \partial M, (n, \ldots, n))$ is generated by $\{U_{n,n,n}^{\otimes v_\Gamma} \otimes U_n^{\otimes v_{\text{inn}}} \otimes e_{\mathbf{i}}\}$, where $\mathbf{i} = (i_1, \ldots, i_{|A|})$ is taken over the $SO(3)$ colorings of A. By Definition 5.18 and Remark 5.16, the first two types of generators satisfy

$$\begin{aligned} |U_n|^2 &= \langle Z'_r(B^3, I, (n)), Z'_r(-B^3, -I, (n))\rangle'_r \\ &= RT'_r(B^3, U, (n)) \\ &= \eta'_r\ [n+1], \text{ and} \\ |U_{n,n,n}|^2 &= \langle Z'_r(B^3, Y, (n, n, n)), Z'_r(-B^3, -Y, (n, n, n))\rangle'_r \\ &= RT'_r(B^3, \theta, (n, n, n)) \\ &= \eta'_r\ \theta(n, n, n), \end{aligned}$$

where U denotes the zero-framed unknot and θ denotes the theta graph. Writing

$$Z'_r(M, L, (n, \ldots, n)) = \sum_{\substack{0 \le \mathbf{i} \le r-3, \\ \mathbf{i} \text{ even}}} \lambda_{\mathbf{i}}\ U_{n,n,n}^{\otimes v_\Gamma} \otimes U_n^{\otimes v_{\text{inn}}} \otimes e_{\mathbf{i}}, \tag{66}$$

we have

$$|Z'_r(M,L,(n,\dots,n))|^2 = (\eta'_r\ \theta(n,n,n))^{v_\Gamma}(\eta'_r\ [n+1])^{v_{\mathrm{inn}}} \sum_{\substack{0\le \mathbf{i}\le r-3,\\ \mathbf{i}\text{ even}}} |\lambda_{\mathbf{i}}|^2 \tag{67}$$

by the orthogonality of $\{e_i\}$. To find $\lambda_{\mathbf{j}}$ for fixed $\mathbf{j}$, we write $\lambda'_{\mathbf{j}} = \lambda_{\mathbf{j}}\,(\eta'^{v_\Gamma+v_{\mathrm{inn}}}_r\ \theta(n,n,n)^{v_\Gamma}[n+1]^{\otimes v_{\mathrm{inn}}})$ and consider

$$\begin{aligned}
\lambda'_{\mathbf{j}} &= \left\langle \sum_{\substack{0\le \mathbf{i}\le r-3,\\ \mathbf{i}\text{ even}}} \lambda_{\mathbf{i}}\ U_{n,n,n}^{\otimes v_\Gamma}\otimes U_n^{\otimes v_{\mathrm{inn}}}\otimes e_{\mathbf{i}}, \overline{U_{n,n,n}^{\otimes v_\Gamma}\otimes U_n^{\otimes v_{\mathrm{inn}}}\otimes e_{\mathbf{j}}} \right\rangle'_r \\
&= \Bigg\langle Z'_r(M,L,(n,\dots,n)) \\
&\qquad \otimes Z'_r(-B^3,-Y,(n,n,n))^{\otimes v_\Gamma}\otimes Z'_r(-B^3,-I,(n))^{\otimes v_{\mathrm{inn}}} \\
&\qquad \otimes Z'_r\left(\bigsqcup_{j=1}^{|A|} -(D^2\times S^1), \bigsqcup_{j=1}^{|A|} -(S^1\times\{0\}), \mathbf{j}\right) \Bigg\rangle'_r \\
&= RT'_r\Bigg(M\cup \bigsqcup_{k=1}^{v_\Gamma+v_{\mathrm{inn}}} B^3 \cup \bigsqcup_{j=1}^{|A|} -(D^2\times S^1), \\
&\qquad\qquad L\cup \bigsqcup_{k=1}^{v_\Gamma} Y \cup \bigsqcup_{k=1}^{v_{\mathrm{inn}}} I \cup \bigsqcup_{j=1}^{|A|} -(S^1\times\{0\}), (n,\dots,n,j_1,\dots,j_{|A|})\Bigg) \\
&= RT'_r(S^3,\Gamma,(n,\dots,n)) \\
&= \eta'_r\langle\Gamma\rangle_n,
\end{aligned}$$

which yields the desired result. □

Remark 6.2. Observe that in the above proof, we only make use of $\mathbf{b}^{(r)}$ when it comes to the zero-color of the extra edges added in Proposition 6.1, not the color n for the original edges of Γ. Indeed, a corresponding version of Main Theorem 2 does hold for any admissible coloring of Γ. We choose to present the theorem for the all-n coloring

purely because the all-n coloring will be significant to the proof of Corollary 1.5 in the next section. We also remark that Proposition 6.1 and Main Theorem 2 hold for (non-augmented) planar KTGs as well. We state only the result, but the proof follows from Theorem 5.17 and the TQFT strategy used above.

Proposition 6.3. *Let $r \geq 3$ be an odd integer and $\Gamma \subset S^2$ a planar KTG with v_Γ vertices colored admissibly by $\boldsymbol{b}_\Gamma^{(r)}$. Let M and $\mathcal{T}$ be defined as in Section 6.1, and let v_{inn} be the number of inner vertices of $\mathcal{T}$. Let $\boldsymbol{b}^{(r)}$ be the admissible coloring of $\mathcal{T}$ induced by $\boldsymbol{b}_\Gamma^{(r)}$. Then,*

$$TV_r(M, \mathcal{T}, \boldsymbol{b}^{(r)}) = 2^{v_\Gamma - 1}(\eta_r')^{2-2v_\Gamma}\theta(n,n,n)^{-v_\Gamma}[n+1]^{-v_{inn}}\left|\langle\Gamma\rangle_{\boldsymbol{b}^{(r)}}\right|^2. \tag{68}$$

6.2 Proof of Corollary 1.5

In this section, we use Main Theorem 2 to verify Conjecture 5.14 for certain choices of $(M, \mathcal{T}, \mathbf{b}^{(r)})$. Let us consider a KTG $\Gamma \subset S^3$, which can be generated from the tetrahedron graph without unzip moves, and let M, $\mathcal{T}$, and $\mathbf{b}^{(r)}$ be defined as in Section 6.1. Note that Γ is already an augmented KTG having zero augmentation rings and $v_{\text{inn}} = 0$. In this scenario, the conclusion of Main Theorem 2 simplifies to

$$TV_r(M, \mathcal{T}, \mathbf{b}^{(r)}) = 2^{v_\Gamma - 1}(\eta_r')^{2-2v_\Gamma}\theta(n,n,n)^{-v_\Gamma}\left|\langle\Gamma\rangle_n\right|^2, \tag{69}$$

so all that remains is to compute $|\langle\Gamma\rangle_n|^2$ and evaluate the limit in (52).

Proof of Corollary 1.5. Let S be a sequence of generating moves for Γ. Write θ_+, θ_-, and t for the number of positive half-twist, negative half-twist, and triangle moves in S, respectively. By reversing the generating moves in S using the relations of Figure

31, we obtain

$$\langle \Gamma \rangle_n = \left((-1)^{\frac{n}{2}} q^{\frac{n^2+2n}{4}}\right)^{\theta_+ - \theta_-} \theta(n,n,n)^{-t} \left\langle \; \right\rangle^{t+1} \quad . \tag{70}$$

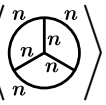

By (69), we must consider

$$\lim_{r\to\infty} \frac{2\pi}{r} \log(2^{v_\Gamma} (\eta'_r)^{2-2v_\Gamma} \theta(n,n,n)^{-v_\Gamma} \, |\langle \Gamma \rangle_n|^2). \tag{71}$$

at $q = e^{\frac{2\pi i}{r}}$ where r ranges over odd integers greater than or equal to 9. By substituting in (70) and observing that η'^{2-2v}_r grows sub-exponentially, this limit equals

$$\lim_{r\to\infty} \frac{2\pi}{r} \log \left(\left| \theta(n,n,n)^{-t-v_\Gamma} \left\langle \; \right\rangle^{t+1} \right|^2 \right). \tag{72}$$

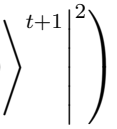

The growth rates of certain $6j$ symbols have been studied extensively in the literature. In [Bel+22, Lemma 3.16], the authors show

$$\lim_{r\to\infty} \frac{2\pi}{r} \log \left(\left| \left\langle \; \right\rangle \right| \right) = v_{\text{oct}}, \tag{73}$$

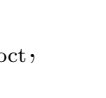

where $v_{\text{oct}} \approx 3.66386$ is the volume of a regular ideal hyperbolic octahedron. We claim that $|\theta(n,n,n)|$ grows sub-exponentially.

Recall from Definition 5.10 that the value of the n-colored theta graph is

$$\theta(n,n,n) = (-1)^{\frac{3n}{2}} \frac{[\frac{3n}{2}+1]!([\frac{n}{2}]!)^3}{([n]!)^3}. \tag{74}$$

Writing $k = \frac{n}{2}$, this becomes

$$\begin{aligned}\theta(n,n,n) &= (-1)^{3k}\frac{[3k+1]!([k]!)^3}{([2k]!)^3} \\ &= (-1)^{3k}\frac{[k]![2k+1]\cdots[3k+1]}{([k+1]\cdots[2k])^2}. \end{aligned} \tag{75}$$

We have different relations depending on the exact value of $n = \frac{r\pm1}{2}$. If $n = \frac{r-1}{2}$, then for all $j \in \mathbb{Z}$ we have

$$\begin{aligned}[k+j] &= \frac{\sin(\frac{2\pi}{r}(\frac{r-1}{4}+j))}{\sin(\frac{2\pi}{r})} \\ &= \frac{\sin(\frac{\pi}{2}+\frac{2\pi}{r}(\frac{-1}{4}+j))}{\sin(\frac{2\pi}{r})} \\ &= \frac{\sin(\frac{\pi}{2}-\frac{2\pi}{r}(\frac{-1}{4}+j))}{\sin(\frac{2\pi}{r})} \\ &= \frac{\sin(\frac{2\pi}{r}(\frac{r+1}{4}-j))}{\sin(\frac{2\pi}{r})} \\ &= [k+\frac{1}{2}-j]. \end{aligned} \tag{76}$$

Note that (76) implies that $[2k+j] = -[2k+1-j]$. Using these, (75) simplifies to

$$\theta(n,n,n) = (-1)^{4k+1}\frac{[k]!}{[\frac{1}{2}][\frac{3}{2}]\cdots[k-\frac{1}{2}]}[k]. \tag{77}$$

Likewise, if $n = \frac{r+1}{2}$, then for all $j \in \mathbb{Z}$ we have

$$[k+j] = [k-\frac{1}{2}-j], \tag{78}$$

and in this case, (75) simplifies to

$$\theta(n,n,n) = (-1)^{4k+2}\frac{[k]!}{[\frac{-1}{2}][\frac{1}{2}]\cdots[k-\frac{3}{2}]}\frac{[k-2][k-1][k]}{[\frac{1}{2}]^2}. \tag{79}$$

In either case, notice that (77) and (79) contain products of the form $\prod_{j=1}^{k} \frac{[j]}{[j-\frac{2\pm1}{2}]}$. By L'Hôpital's Rule,

$$\begin{aligned}\lim_{r\to\infty} \frac{[j]}{[j-\frac{2\pm1}{2}]} &= \lim_{r\to\infty} \frac{\sin(\frac{2\pi}{r}j)}{\sin(\frac{2\pi}{r}(j-\frac{2\pm1}{2}))} \\ &= \lim_{r\to\infty} \frac{-\frac{2\pi}{r^2}j}{-\frac{2\pi}{r^2}(j-\frac{2\pm1}{2})} \frac{\cos(\frac{2\pi}{r}j)}{\cos(\frac{2\pi}{r}(j-\frac{2\pm1}{2}))} \\ &= \frac{j}{j-\frac{2\pm1}{2}} \end{aligned} \tag{80}$$

for fixed j. Observe also that the term-wise sequences are monotone increasing. Therefore, we have

$$\begin{aligned}\lim_{r\to\infty} \frac{2\pi}{r} \sum_{j=1}^{k} \log\left(\frac{[j]}{[j-\frac{2\pm1}{2}]}\right) &\leq \lim_{r\to\infty} \frac{2\pi}{r} \sum_{j=1}^{k} \log\left(\frac{j}{j-\frac{2\pm1}{2}}\right) \\ &= \lim_{r\to\infty} \frac{2k\pi}{r} \mathrm{Ave}\left\{ \log\left(\frac{j}{j-\frac{2\pm1}{2}}\right)\right\}_{j=1}^{k}, \end{aligned} \tag{81}$$

where $\mathrm{Ave}\{s_j\}_{n=j}^{k}$ denotes the average of the finite sequence $\{s_j\}_{n=j}^{k}$. As the sequence $\left\{ \log\left(\frac{j}{j-\frac{2\pm1}{2}}\right)\right\}_{j=1}^{\infty}$ converges to zero as $j \to \infty$, its average also converges to zero as $k \to \infty$. Thus, the limit in (81) vanishes as claimed. Next, we claim that the same happens for the remaining terms in (77) and (79). Indeed, by L'Hôpital's Rule we have in particular that

$$\begin{aligned}\lim_{r\to\infty} \frac{2\pi}{r} \log([k]) &= \lim_{r\to\infty} 2\pi \frac{\frac{d}{dr}[k]}{[k]} \\ &= \lim_{r\to\infty} 2\pi \frac{\frac{\pi}{2}(\mp\frac{1}{r^2})\cos(\frac{2\pi}{r}(\frac{r\pm1}{4}))}{\sin(\frac{2\pi}{r}(\frac{r\pm1}{4}))} + \frac{\frac{2\pi}{r}\cos(\frac{2\pi}{r})}{\frac{r}{2\pi}\sin(\frac{2\pi}{r})} \\ &= 0. \end{aligned} \tag{82}$$

We can similarly show that the terms $[k-1]$ and $[k-2]$ in (79) also grow sub-exponentially. We conclude that

$$\lim_{r\to\infty} \frac{2\pi}{r} \log(TV_r'(M, \mathcal{T}, \mathbf{b}^{(r)})) = (2t+2)v_{\text{oct}}. \tag{83}$$

To prove Corollary 1.5, we must show this is the volume of the manifold M_{E_θ}, which is M equipped with the hyperbolic polyhedral metric $(M, \mathcal{T})$ having cone angles $\theta = (\theta_1, \cdots, \theta_{|E|})$ determined by the choice of coloring. For $\mathbf{b}^{(r)} = (n, \ldots, n)$ these are

$$\theta_i = \left| 2\pi - \lim_{r\to\infty} \frac{4\pi n}{r} \right| = 0. \tag{84}$$

Recall that a geodesic edge with cone angle zero is precisely an annular cusp. Thus, M_{E_θ} is homeomorphic to the outside of Γ, O_Γ. By Proposition 5.23, we have $\text{Vol}(M_{E_\theta}) = (2t+2)v_{\text{oct}}$, which agrees with (83). □

6.3 Discussion of results

In the case where the KTG Γ is planar, such as in the statement of Corollary 1.5, Conjecture 1.2 can be viewed as a Turaev–Viro analogue of the volume conjecture for polyhedra stated in [CGV15, Conjecture 1.3]. The volume conjecture for polyhedra asserts that taking the limit of the colored Jones evaluations of a planar KTG at the classical root of unity $q = e^{\frac{\pi i}{r}}$ yields the volume of a single hyperbolic polyhedron with cone angles determined in the same manner as in Conjecture 5.14. Since a polyhedral decomposition of M_{E_θ} can be obtained by taking two copies of such a polyhedron, one above and one below the projection plane as in the proof of Proposition 6.1, the volumes predicted by the two conjectures differ by a factor of 2. In this light,

Corollary 1.5 can be viewed as an analogue of [CGV15, Theorem 1.4], albeit for only the all-n coloring. In addition to focusing on different roots of unity, the two methods of proof are vastly different. Rather than using Turaev–Viro invariants or TQFTs, the authors of [CGV15] prove their result using the shadow state-sum formulation of the colored Kauffman bracket, a result first appearing in [KR89] which was later expanded upon by Turaev [Tur91].

Indeed, shadow-state sums do provide an alternate method of proof for the planar version of Main Theorem 2 (Proposition 6.3), in lieu of using Theorem 5.17 and the Reshetikhin-Turaev TQFT. Recall that in general, the relative Turaev–Viro invariants depend on the choice of triangulation $\mathcal{T}$ and colors $\{\mathbf{b}^{(r)}\}$, and as such are not 3-manifold invariants. However, it can be shown using handle slides that the chain-mail link constructed in the proof of Theorem 5.17 is unaffected by the addition or removal of zero-colored edges and the coning procedure used in Proposition 6.1. Consequently, one can instead construct the chain-mail link using the handle decomposition dual to the standard polyhedral decomposition of S^3 corresponding to Γ. Since this consists precisely of two polyhedra with faces identified in pairs, one may apply the fusion rule to the ϵ-curves rather than the δ-curves as we did in the proof of Theorem 5.17. The relations of Figure 31 then lead one to recover the shadow-state sum formula. This connection has previously been observed by Kevin Walker from a TQFT perspective, but it is still interesting to note that Yang's chain-mail link realizes this formula.

Bibliography

[Bel+22] Giulio Belletti et al. "Growth of quantum $6j$-symbols and applications to the volume conjecture". *J. Differential Geom.* 120.2 (2022), pp. 199–229.

[BK22a] Brandon Bavier and Efstratia Kalfagianni. "Guts, volume and Skein Modules of 3-manifolds". *Fund. Math.* 256 (2022), pp. 195–220.

[BK22b] Hans U. Boden and Homayun Karimi. "The Jones–Krushkal polynomial and minimal diagrams of surface links". *Ann. Inst. Fourier* 72.4 (2022), pp. 1437–1475.

[Bla+95] C. Blanchet et al. "Topological quantum field theories derived from the Kauffman bracket". *Topology* 34.4 (1995), pp. 883–927.

[Bon21] Joe Boninger. *A Quantum Invariant of Links in $T^2 \times I$ with Volume Conjecture Behavior*. 2021. arXiv: `2012.07782 [math.GT]`.

[Bur] Benjamin A. Burton. "The next 350 million knots". *36th International Symposium on Computational Geometry*. Vol. 164. LIPIcs. Leibniz Int. Proc. Inform. Art. No. 25, 17.

[CGV15] Francesco Constantino, Francois Gueritaud, and Roland van der Veen. "On the volume conjecture for polyhedra". *Geometriae Dedicata* 179.1 (2015), pp. 385–409.

[CK22] Abhijit Champanerkar and Ilya Kofman. "A volumish theorem for alternating virtual links". *New York J. Math.* 28 (2022), pp. 337–356.

[CY18] Qingtao Chen and Tian Yang. "Volume conjectures for the Reshetikhin-Turaev and the Turaev-Viro invariants". *Quantum Topol.* 9.3 (2018), pp. 419–460.

[DKY18] Renaud Detcherry, Efstratia Kalfagianni, and Tian Yang. "Turaev-Viro invariants, colored Jones polynomials, and volume". *Quantum Topol.* 9.4 (2018), pp. 775–813.

[DL06] Oliver T. Dasbach and Xiao-Song Lin. "On the head and the tail of the colored Jones polynomial". *Compos. Math.* 142.5 (2006), pp. 1332–1342.

[DL07] Oliver T. Dasbach and Xiao-Song Lin. "A volume-ish theorem for the Jones polynomial of alternating knots". *Pacific J. Math.* 231.2 (2007), pp. 279–291.

[FK22] Paul Fendley and Vyacheslav Krushkal. "Topological quantum field theory and polynomial identities for graphs on the torus". *Ann. Inst. Henri Poincaré* (2022).

[FKP08] David Futer, Efstratia Kalfagianni, and Jessica S. Purcell. "Dehn filling, volume, and the Jones polynomial". *J. Differential Geom.* 78.3 (2008), pp. 429–464.

[Jon85] Vaughan F. R. Jones. "A polynomial invariant for knots via von Neumann algebras". *Bull. Amer. Math. Soc. (N.S.)* 12.1 (1985), pp. 103–111.

[Kas95] R. M. Kashaev. "A link invariant from quantum dilogarithm". *Modern Phys. Lett. A* 10.19 (1995), pp. 1409–1418.

[Kau87] Louis H. Kauffman. "State models and the Jones polynomial". *Topology* 26.3 (1987), pp. 395–407.

[KP20] Efstratia Kalfagianni and Jessica S. Purcell. *Alternating links on surfaces and volume bounds*. to appear in Communications in Analysis and Geometry. 2020. arXiv: `2004.10909 [math.GT]`.

[KR89] A. N. Kirillov and N. Yu. Reshetikhin. "Representations of the algebra $U_q(\mathrm{sl}(2))$, q-orthogonal polynomials and invariants of links". *Infinite-dimensional Lie algebras and groups (Luminy-Marseille, 1988)*. Vol. 7. Adv. Ser. Math. Phys. World Sci. Publ., Teaneck, NJ, 1989, pp. 285–339.

[Kru11] Vyacheslav Krushkal. "Graphs, links, and duality on surfaces". *Combin. Probab. Comput.* 20.2 (2011), pp. 267–287.

[Lac04] Marc Lackenby. "The volume of hyperbolic alternating link complements". *Proc. London Math. Soc. (3)* 88.1 (2004). With an appendix by Ian Agol and Dylan Thurston, pp. 204–224.

[Lic62] W. B. R. Lickorish. "A representation of orientable combinatorial 3-manifolds". *Ann. of Math. (2)* 76 (1962), pp. 531–540.

[Lic97] W. B. Raymond Lickorish. *An introduction to knot theory*. Vol. 175. Graduate Texts in Mathematics. Springer-Verlag, New York, 1997, pp. x+201.

[MM01] Hitoshi Murakami and Jun Murakami. "The colored Jones polynomials and the simplicial volume of a knot". *Acta Math.* 186.1 (2001), pp. 85–104.

[Mur11] Hitoshi Murakami. "An introduction to the volume conjecture". *Interactions between hyperbolic geometry, quantum topology and number theory*. Vol. 541. Contemp. Math. Amer. Math. Soc., Providence, RI, 2011, pp. 1–40.

[Mur87] Kunio Murasugi. "Jones polynomials and classical conjectures in knot theory". *Topology* 26.2 (1987), pp. 187–194.

[MV94] G. Masbaum and P. Vogel. “3-valent graphs and the Kauffman bracket”. *Pacific J. Math.* 164.2 (1994), pp. 361–381.

[Pie88] Riccardo Piergallini. “Standard moves for standard polyhedra and spines”. 18. Third National Conference on Topology (Italian) (Trieste, 1986). 1988, pp. 391–414.

[Pra73] Gopal Prasad. “Strong rigidity of **Q**-rank 1 lattices”. *Invent. Math.* 21 (1973), pp. 255–286.

[Prz91] Józef H. Przytycki. “Skein modules of 3-manifolds”. *Bull. Polish Acad. Sci. Math.* 39.1-2 (1991), pp. 91–100.

[Pur20] Jessica S. Purcell. *Hyperbolic knot theory*. Vol. 209. Graduate Studies in Mathematics. American Mathematical Society, Providence, RI, 2020, pp. xviii+369.

[Rob95] Justin Roberts. “Skein theory and Turaev-Viro invariants”. *Topology* 34.4 (1995), pp. 771–787.

[Sto06] Alexander Stoimenow. *Non-triviality of the Jones polynomial and the crossing numbers of amphicheiral knots*. 2006. arXiv: `math/0606255 [math.GT]`.

[Thi87] Morwen B. Thistlethwaite. “A spanning tree expansion of the Jones polynomial”. *Topology* 26.3 (1987), pp. 297–309.

[Thu82] William P. Thurston. “Three-dimensional manifolds, Kleinian groups and hyperbolic geometry”. *Bull. Amer. Math. Soc. (N.S.)* 6.3 (1982), pp. 357–381.

[Thu97] William P. Thurston. *Three-dimensional geometry and topology. Vol. 1*. Vol. 35. Princeton Mathematical Series. Edited by Silvio Levy. Princeton University Press, Princeton, NJ, 1997, pp. x+311.

[Tur91] Vladimir G. Turaev. “State sum models in low-dimensional topology”. *Proceedings of the International Congress of Mathematicians, Vol. I, II (Kyoto, 1990)*. Math. Soc. Japan, Tokyo, 1991, pp. 689–698.

[TV92] V. G. Turaev and O. Ya. Viro. “State sum invariants of 3-manifolds and quantum $6j$-symbols”. *Topology* 31.4 (1992), pp. 865–902.

[Vee09] Roland van der Veen. “The volume conjecture for augmented knotted trivalent graphs”. *Algebr. Geom. Topol.* 9.2 (2009), pp. 691–722.

[Wal60] Andrew H. Wallace. “Modifications and cobounding manifolds”. *Canadian J. Math.* 12 (1960), pp. 503–528.

[Wil22] David A. Will. “Homological Polynomial Coefficients and the Twist Number of Alternating Surface Links”. *Algebr. Geom. Topol.* 22.8 (2022), pp. 3939–3963.

[Yan21] Tian Yang. *A relative version of the Turaev-Viro invariants and the volume of hyperbolic polyhedral 3-manifolds*. 2021. arXiv: `2009.04813 [math.GT]`.